Drug-based modulation of endogenous stem cells promotes functional remyelination in vivo

Fadi J. Najm[1], **Mayur Madhavan**[1], **Anita Zaremba**[2], **Elizabeth Shick**[1], **Robert T. Karl**[1], **Daniel C. Factor**[1], **Tyler E. Miller**[1,3,4], **Zachary S. Nevin**[1], **Christopher Kantor**[2], **Alex Sargent**[2], **Kevin L. Quick**[5], **Daniela M. Schlatzer**[6], **Hong Tang**[7], **Ruben Papoian**[7,+], **Kyle R. Brimacombe**[8], **Min Shen**[8], **Matthew B. Boxer**[8], **Ajit Jadhav**[8], **Andrew P. Robinson**[9], **Joseph R. Podojil**[9], **Stephen D. Miller**[9], **Robert H. Miller**[2,#,*], and **Paul J. Tesar**[1,2,*]

[1]Department of Genetics and Genome Sciences, Case Western Reserve University School of Medicine, Cleveland, Ohio 44106, USA

[2]Department of Neurosciences, Case Western Reserve University School of Medicine, Cleveland, Ohio 44106, USA

[3]Department of Pathology, Case Western Reserve University School of Medicine, Cleveland, Ohio 44106, USA

[4]Department of Stem Cell Biology and Regenerative Medicine, Lerner Research Institute, Cleveland Clinic, Cleveland, Ohio 44195, USA

[5]PerkinElmer, Waltham, Massachusetts 02451, USA

[6]Center for Proteomics and Bioinformatics, Case Western Reserve University School of Medicine, Cleveland, Ohio 44106, USA

[7]Drug Discovery Center, University of Cincinnati College of Medicine, Cincinnati, Ohio 45237, USA

[8]National Center for Advancing Translational Sciences, National Institutes of Health, 9800 Medical Center Drive, Rockville, MD, 20850, USA

[9]Department of Microbiology-Immunology and Interdepartmental Immunobiology Center, Feinberg School of Medicine, Northwestern University, 303 E. Chicago Avenue, Chicago, IL 60611, USA

Abstract

Multiple sclerosis (MS) involves an aberrant autoimmune response and progressive failure of remyelination in the central nervous system (CNS). Prevention of neural degeneration and subsequent disability requires remyelination through the generation of new oligodendrocytes, but current treatments exclusively target the immune system. Oligodendrocyte progenitor cells (OPCs) are stem cells in the CNS and the principal source of myelinating oligodendrocytes[1]. OPCs are abundant in demyelinated regions of MS patients, yet fail to differentiate, thereby representing a cellular target for pharmacological intervention[2]. To discover therapeutic compounds for enhancing myelination from endogenous OPCs, we screened a library of bioactive small molecules on mouse pluripotent epiblast stem cell (EpiSC)-derived OPCs[3–5]. We identified seven drugs that functioned at nanomolar doses to selectively enhance the generation of mature oligodendrocytes from OPCs *in vitro*. Two drugs, miconazole and clobetasol, were effective in promoting precocious myelination in organotypic cerebellar slice cultures, and *in vivo* in early postnatal mouse pups. Systemic delivery of each of the two drugs significantly increased the number of new oligodendrocytes and enhanced remyelination in a lysolecithin-induced mouse model of focal demyelination. Administering each of the two drugs at the peak of disease in the experimental autoimmune encephalomyelitis (EAE) mouse model of chronic progressive MS resulted in striking reversal of disease severity. Immune response assays showed that miconazole functioned directly as a remyelinating drug with no effect on the immune system, whereas clobetasol was a potent immunosuppressant as well as a remyelinating agent. Mechanistic studies showed that miconazole and clobetasol functioned in OPCs through mitogen-activated protein kinase (MAPK) and glucocorticoid receptor (GR) signaling, respectively. Furthermore, both drugs enhanced the generation of human oligodendrocytes from human OPCs *in vitro*. Collectively, our results provide a rationale for testing miconazole and clobetasol, or structurally-modified derivatives, to enhance remyelination in patients.

As repair of damaged myelin may provide therapeutic benefit in MS and other demyelinating disorders[6–12], we set out to identify drugs that could be repurposed as remyelinating therapeutics. We selected the NIH Clinical Collection I and II libraries comprised of 727 drugs with a history of safe use in clinical trials, to test for maturation of OPCs into myelinating oligodendrocytes. Using mouse EpiSC-derived OPCs, we developed an *in vitro* phenotypic screen that accurately quantified differentiation into mature oligodendrocytes by high content imaging of myelin protein expression (Fig. 1a).

Two batches (>100 million cells each) of pure OPCs were generated from independent mouse pluripotent EpiSC lines of opposite sex (Extended Data Fig. 1a). EpiSC-derived OPCs shared virtually all defining molecular and cellular properties including gene expression profiles with *in vivo* isolated OPCs but provided the key advantage of being highly scalable (Extended Data Fig. 1b)[3]. For *in vitro* screening, the seeding density, endpoint assays, and DMSO (vehicle) tolerance were optimized in pilot studies to assure

accurate and reproducible measurement of OPC differentiation in a 96-well format (Extended Data Fig. 1c).

For the primary screen, OPCs were treated with vehicle alone (0.05% (v/v) DMSO) as a negative control, thyroid hormone (a known OPC differentiation inducer) as a positive control[13], or drug dissolved in DMSO at a concentration of 5 μM. After 72 hours, cells were fixed and labeled with antibodies to myelin basic protein (MBP) and the length and intensity of MBP labeled oligodendrocyte processes measured (Fig. 1a). These features were reliable indicators of alteration in cellular phenotype, as indicated by consistency and high signal to background ratio of positive and vehicle controls across all screening plates (Extended Data Fig. 1d–g). We then normalized the experimental data for the tested drugs against thyroid hormone (set value of 100) on a per plate basis. Based on this analysis, we identified the 22 drugs that enhanced oligodendrocyte formation greater than five standard deviations above DMSO treatment and also outperformed thyroid hormone in the measured parameters (Fig. 1b). Notably, one of the top 22 drugs was benztropine, a muscarinic receptor antagonist recently shown to induce OPC differentiation and remyelination[8,9].

To validate and prioritize the 22 drug hits, the assay was repeated using alternate OPCs, reagents, and parameters to eliminate screen-specific artifacts (see Methods). Drugs were ranked by their dose-dependent ability to induce oligodendrocyte generation from OPCs without toxicity (Extended Data Fig. 2a). To demonstrate reproducibility, an independent laboratory tested selected drug hits using distinct equipment, plate format (1536-well), personnel, and imaging/analysis scripts (see Methods). Of the 16 hits tested at the external screening site, 14 were validated as potent inducers of oligodendrocyte differentiation (Extended Data Fig. 2a, b).

We next tested whether the drug hits could promote the maturation of native OPCs in CNS tissue. Cerebellar slices were generated from postnatal day seven mice—a time that precedes widespread myelination—and treated *ex vivo* with drug or DMSO (vehicle) for five days and labeled with anti-MBP antibodies (Fig. 1c)[6,7]. We screened eleven of the top drugs and used an in house-developed high content analysis algorithm to rank them based on their ability to increase the extent of MBP+ aligned fibers in whole cerebellar slices. The 'high' performing group consisted of four drugs that increased the number of MBP+ aligned fibers ~150% or greater (Fig. 1d and Extended Data Fig. 2a). We validated the accuracy of our high content screen by semi-quantitative western blotting of MBP protein isoforms in independent slice culture experiments (Fig. 1d, e)[14,15].

Structure-activity-relationship analysis revealed that the top hits from the primary screen segregated into two specific classes containing either a (1,3) diazole with mono-substitution at the 1-position or a sterane base structure (Extended Data Fig. 3a–d). We selected miconazole and clobetasol, the top overall performing hits in each of the imidazole and sterane classes respectively, for further mechanistic and functional testing after confirming that both drugs readily crossed the blood brain barrier in mice (Fig. 1f, Extended Data Fig. 2a, and Supplementary Table 1). Miconazole is a topical antifungal agent functioning through cytochrome P450 inhibition and clobetasol is a potent topical corticosteroid, but their functions in OPCs were unknown.

To test if miconazole or clobetasol enhance remyelination *in vivo*, we used a toxin-induced model whereby focal demyelinated lesions are generated in spinal cord dorsal white matter of adult mice by localized injection of lysolecithin (LPC). In lesioned animals, demyelination is complete within four days, after which OPCs are recruited into the lesion. Widespread remyelination does not normally commence until 14–21 days post lesion (dpl), which provides a defined window from days 4–14 to test the efficacy of drugs to enhance the extent and rate of remyelination[16]. Both miconazole (10 or 40 mg/kg) and clobetasol (2 mg/kg) treatment induced a marked improvement within the lesions of treated mice as compared to vehicle treated controls. At eight dpl both drugs induced a significant increase in the number of newly generated CC1+ oligodendrocytes in the lesion core (Fig. 2a, b). This was coincident with extensive MBP staining in the lesions of miconazole- and clobetasol- but not vehicle-treated animals at both eight and twelve dpl (Fig. 2a). Toluidine blue stained sections and electron micrographs demonstrated that miconazole and clobetasol each induced a striking increase in the extent of remyelination (Fig. 2c, d and Extended Data Fig. 4a, b). At twelve dpl, lesions of vehicle-treated mice consisted mostly of unmyelinated axons (6% myelinated) while those of clobetasol- and miconazole-treated mice contained >70% remyelinated axons throughout the extent of the lesion (Fig. 2d). Analysis of myelin thickness relative to axon diameter (g-ratio) at twelve dpl revealed that miconazole- and clobetasol-induced myelin was thinner than intact myelin, a defining characteristic of remyelination (Fig. 2d).

We also evaluated whether miconazole or clobetasol could promote precocious myelination during development, in the absence of injury or disease. We treated postnatal day two mice —a time point that precedes widespread CNS myelination—daily for four days with drug or vehicle. In miconazole- and clobetasol-treated mice, we found a significant increase in the number of CC1+ oligodendrocytes in the lateral corpus callosum as compared to vehicle-treated mice (Extended Data Fig. 5a). Additionally, we found a significantly larger portion of the corpus callosum was populated by MBP+ fiber tracts in miconazole- and clobetasol-treated mice (Extended Data Fig. 5b). This suggests that clobetasol and miconazole enhance myelination in the absence of damage or disease. Collectively, the LPC demyelination and developmental mouse models demonstrate that miconazole and clobetasol each function to induce the differentiation of endogenous OPCs in the CNS and promote enhanced myelination.

To determine if the drugs were working at a particular stage of the OPC differentiation process, we seeded OPCs in differentiation conditions and treated them with either miconazole or clobetasol at different time points (0, 16, 24, or 48 hour), and assayed MBP expression at 72 hours. For both miconazole and clobetasol, the number of MBP+ oligodendrocytes present at 72 hours was dependent on drug treatment within the first 24 hours of differentiation (Fig. 3a). In agreement with this data, treatment of differentiating OPCs with either drug for different durations (24, 48, 56, and 72 hours) induced a progressive, time-dependent increase in the number of MBP+ oligodendrocytes (Fig. 3b). These data suggest that both drugs function directly on OPCs early in the differentiation process. Additionally, neither drug showed a significant impact on astrocyte formation from

OPCs *in vitro*, suggesting they likely function as direct inducers of oligodendrocyte differentiation (Fig. 3c).

Muscarinic receptor antagonists such as benztropine and clemastine have recently been identified as remyelinating agents[8,9]. Therefore we tested whether miconazole or clobetasol function through the muscarinic acetylcholine pathway using functional cellular reporter assays of all muscarinic receptor subtypes (M1–M5). Neither miconazole nor clobetasol inhibited any of the five muscarinic receptor subtypes (Fig. 3d). We then profiled whether clobetasol or miconazole biochemically inhibited the activity of 414 different kinase isoforms. Neither clobetasol nor miconazole inhibited any of the kinases tested, suggesting their activity is not based on direct inhibition of protein kinases (Supplementary Table 2).

To explore the signaling pathways in OPCs influenced by these drugs, we performed genome-wide RNAseq and phosphoproteomic analyses on mouse OPCs treated with drug or vehicle (Extended Data Fig. 6a–d and Supplementary Table 3). Miconazole or clobetasol treatment altered OPC transcript expression and phosphoproteins within hours, and influenced expression of genes in signaling pathways involved in oligodendrocyte maturation and myelination. Clobetasol potently modulated genes downstream of multiple nuclear hormone receptors, including GR, which are known to be important regulators of myelin gene expression[13,17]. Since GR signaling is also known to enhance Schwann cell-mediated myelination in the peripheral nervous system[18], we tested if clobetasol's activity on OPCs was mediated by GR signaling. Treatment of OPCs with clobetasol for one hour increased the phosphorylation of GR at Ser220, an activating post-translational modification (Fig. 3e). RU486, a competitive GR antagonist, blocked clobetasol-induced GR phosphorylation and oligodendrocyte differentiation (Fig. 3e, f) suggesting that clobetasol's activity in OPCs is mediated through the GR signaling axis.

For miconazole, pathway analyses showed that proteins in the MAPK pathway were most strongly impacted (Extended Data Figure 7a, b and Supplementary Table 3). Most prominent was the strong and sustained phosphorylation of both ERK1 and ERK2 (ERK1/2) at canonical activation sites which we validated by western blotting (Fig. 3g). In mice, genetic loss of ERK1/2 in the oligodendrocyte lineage results in normal numbers of OPCs and oligodendrocytes but widespread hypomyelination, while constitutive activation of ERK1/2 results in a profound increase in the extent of remyelination after toxin-induced demyelinating injury[19,20]. In contrast to miconazole, treatment of OPCs with clobetasol or benztropine did not induce ERK1/2 phosphorylation (Fig. 3g). Miconazole treatment of a non-neural cell type, mouse fibroblasts, also showed no increase of ERK1/2 phosphorylation, indicating potential cell type specificity (Fig. 3g). PD0325901, a small molecule inhibitor of ERK's upstream kinase MEK, blocked the ability of miconazole to induce ERK1/2 phosphorylation, suggesting that miconazole functions through a MEK-dependent mechanism in OPCs (Fig. 3h). We also treated mouse OPCs with voriconazole, a triazole-containing antifungal cytochrome P450 inhibitor with 80% structural similarity to miconazole, which failed to induce changes in ERK1/2 phosphorylation (Fig. 3g). This was consistent with the observation that voriconazole did not promote the differentiation of OPCs into oligodendrocytes, and taken together suggests that miconazole's effect on OPCs is independent of cytochrome P450 inhibition (Extended Data Fig. 7c).

We then assessed whether clobetasol and miconazole treatment would enhance the differentiation of human OPCs into oligodendrocytes. We generated human OPCs from human embryonic stem cells (hESCs) and human induced pluripotent stem cells (hiPSCs) (Extended Data Fig. 8a–c)[21,22]. We then treated human OPCs with DMSO, clobetasol, or miconazole for 21 days followed by staining for MBP, imaging and high content analysis (Extended Data Fig. 8d–g). Both drugs enhanced human OPC differentiation, with miconazole exhibiting the most reproducible and potent effects.

To interpret the potential impact of clobetasol or miconazole as therapeutics in immune-mediated MS models, we tested effects on immune cell survival and function. We found that only clobetasol, as expected from its known corticosteroid properties, altered naïve T cell differentiation and both the proliferation and secretion of cytokines by $PLP_{139-151}$ or MOG_{35-55} sensitized lymph node cells (Extended Data Fig. 9a–j). As such, only clobetasol, but not the solely remyelinating drugs miconazole or benztropine, showed efficacy in reducing disease severity in the immune-driven relapsing-remitting $PLP_{139-151}$ EAE model (Fig. 4a). The positive effect of clobetasol in this model resulted from its immunosuppressive effects as evidenced by the severe reduction of T cells within the spleen (Fig. 4b).

We also employed a second EAE mouse model, MOG_{35-55}-induced, in which the immune response is relatively controlled and disease pathology recapitulates chronic progressive demyelination. We used a therapeutic, rather than prophylactic, treatment paradigm to evaluate whether drugs could reverse, rather than prevent disease. Miconazole and clobetasol treated animals all exhibited a marked improvement in function with nearly all animals regaining use of one or both hind limbs (Fig. 4c, d). In contrast, vehicle-treated mice exhibited chronic hind limb paralysis over the treatment period. Benztropine treatment also resulted in functional improvement, but to a lesser extent than miconazole and clobetasol (Fig. 4c, d). Overt functional recovery of miconazole- and clobetasol-treated mice correlated with histological improvements in the spinal cord. Specifically, drug-treated mice showed restoration of MBP expression and a reduction in the extent of demyelination in the spinal cord, whereas vehicle-treated mice showed sustained areas of white matter disruption (Extended Data Fig. 10a–e).

Although clobetasol's immunosuppressive effect makes it challenging to directly evaluate its remyelinating potential in EAE, its consistent and robust induction of OPC differentiation *in vitro*, and enhancement of remyelination in non-immune driven *in vivo* assays suggests that it serves a role in both immunomodulation and promotion of myelination. In contrast, miconazole did not modulate immune cell function and our data indicate that it acts as a direct remyelinating agent. Given the potential of miconazole as a remyelinating therapeutic, we contracted a separate laboratory to provide independent validation of its efficacy in the MOG_{35-55}-induced EAE preclinical model. The laboratory independently validated the preclinical efficacy of miconazole in MOG_{35-55}-induced EAE to reduce disease severity in treated mice (Fig. 4d).

Since the approval in 1993 of interferon beta-1b for the treatment of MS, therapeutic development has centered on the generation of additional immunomodulatory agents.

Despite the effectiveness of many of these drugs to modulate CNS inflammation in MS patients, none of them prevent chronic progressive disease and disability—largely due to their inability to stop or reverse the failure of remyelination in the CNS. We developed an advanced high throughput screening platform to discover effective remyelinating therapeutics. This pluripotent stem cell-based system provides unprecedented scalability, purity, and genotypic-flexibility to screen for compounds that enhance OPC differentiation and myelination. Using this platform we identified two FDA-approved drugs, miconazole and clobetasol, with newly discovered functions to directly modulate OPC differentiation, enhance remyelination, and significantly reduce disease severity in mouse models of MS. Since miconazole and clobetasol are currently only approved for topical administration in humans, significant optimization of dosing, delivery, and potentially chemical structure will be required to enhance the on-target pharmacology in OPCs while diminishing any potential off-target side effects. However, the ability of miconazole and clobetasol to each cross the blood-brain-barrier raises the exciting possibility that these drugs, or modified derivatives, could advance into clinical trials for the currently untreatable chronic progressive phase of MS.

METHODS

Mouse OPC preparation

OPCs used in this study were generated from two separate EpiSC lines, EpiSC9 (female) and 129O1 (male), using *in vitro* differentiation protocols and culture conditions described previously[3,23]. Cultures were regularly tested and shown to be mycoplasma free. To ensure uniformity throughout all *in vitro* screening experiments, EpiSC-derived OPCs were sorted to purity by fluorescent activated cell sorting at passage five with conjugated CD140a-APC (eBioscience, 17–1401; 1:80) and NG2-AF488 (Millipore, AB5320A4; 1:100) antibodies. Sorted batches of OPCs were expanded and frozen down in aliquots. OPCs were thawed into growth conditions for one passage prior to use in screening assays.

in vitro phenotypic screening of OPCs

EpiSC-derived OPCs were seeded onto poly-D-lysine 96 well Viewplate or CellCarrier plates (PerkinElmer) coated with laminin (Sigma, L2020; 10μg/ml) using electronic multichannel pipetors. For the primary screen, 30,000 cells were seeded per well in screening medium [DMEM/F12 supplemented with N2 (R&D Systems), B-27 (Life Technologies), neurotrophin 3 (R&D Systems; 10ng/ml), cAMP (Sigma; 50μM), IGF-1 (R&D Systems; 100ng/ml), noggin (R&D Systems; 100ng/ml)] and allowed to attach for two hours prior to addition of drug. NIH Clinical Collection I and II (http://www.nihclinicalcollection.com) drugs were added to assay plates with 0.1μl pin replicators (Molecular Devices, Genetix; X5051) resulting in a final primary screening concentration of 5 μM. Thyroid hormone positive controls and DMSO vehicle controls were included in each assay plate. Cells were incubated under standard conditions (37°C, 5% CO_2) for three days and fixed with 4% paraformaldehyde (PFA) in phosphate buffered saline (PBS). Fixed plates were permeabilized with 0.1% Triton X-100 and blocked with 10% donkey serum (v/v) in PBS for two hours. Cells were labeled with MBP antibodies (Abcam, ab7349; 1:100) for one hour at room temperature followed by detection with Alexa Fluor-conjugated

secondary antibodies (1:500) for 45 minutes. Nuclei were visualized by DAPI staining (Sigma; 1 μg/ml). All plates for the primary screen were processed and analyzed simultaneously to eliminate variability. Donepezil was identified in the primary screen however the drug was not available at the time of dose response testing and was excluded from further testing.

Dose response testing of drugs hits followed the same procedure with the following modifications to eliminate any artifacts in the primary screen: independently-sourced drugs; a distinct batch of EpiSC-derived OPCs from a mouse of opposite sex; multi-dose testing; cytotoxicity analysis; an alternate marker of mature oligodendrocytes proteolipid protein 1 (PLP1, antibody clone AA3 kindly provided by Bruce Trapp; 1:5,000); and an alternate high content assay endpoint parameter (percent of oligodendrocytes differentiated instead of process intensity and length parameters). All drugs were tested in quadruplicate at seven different doses (ranging from 333 nM to 6.7 μM) and classified into tiers based on their EC_{50} to induce OPC maturation, and their toxicity (concentration at which 50% of the cells were lost). Tier A drugs (n = 3) consisted of nanomolar dose effectors with little to no detectable toxicity at doses tested. Tier B drugs (n = 4) showed nanomolar effects but demonstrated toxicity at high doses. Tier C and D drugs required high doses to see an effect, demonstrated toxicity at low doses, or failed to show a dose dependent response.

High content analysis of *in vitro* screen

For the 5 μM *in vitro* screen, stained plates were imaged on the Opera® confocal imaging system (PerkinElmer) and a set of 24 10× fields were collected from each well resulting in an average of 10,000 cells being scored per well. For the dose response (6.7 μM, 5 μM, 3.3 μM, 1.7 μM, 666 nM, 500 nM, and 333 nM) *in vitro* assays, plates were imaged on the Operetta® High Content Imaging and Analysis system (PerkinElmer) and a set of 14 20× fields captured from each well resulting in an average of 3,300 cells being scored per well. Analysis (PerkinElmer Acapella®, Harmony®, and Columbus™ software) began by identifying intact nuclei stained by DAPI; i.e. those traced nuclei that were larger than 50 μm^2 in surface area and possessed intensity levels that were typical and less than the threshold brightness of pyknotic cells. Each traced nucleus region was then expanded by 50% and cross referenced with the mature myelin protein (MBP or PLP1) stain to identify oligodendrocyte nuclei, and from this percent of oligodendrocytes was calculated. Processes emanating from oligodendrocyte nuclei were identified using the CSIRO2 analysis module within a custom Acapella® script. Maximum mean process length (denoted "process length") and mean process intensity (denoted "process intensity") were generated on a per well basis. For the 5 μM *in vitro* screen, values were calculated and normalized to 100 for thyroid hormone (positive control) treated wells and to 0 for DMSO (vehicle) treated wells, on a per plate basis.

1536-well phenotypic validation testing of OPCs

Briefly, OPCs were grown and expanded in laminin-coated flasks before harvesting for plating. Cells were dispensed in screening media (see above for details) using a Multidrop Combi dispenser (Thermo Fisher) into laminin/poly-L-ornithine-coated sterile, 1536-well, black clear-bottom tissue culture plates (Brooks Automation), to a final density of 2,000

cells/well. Plates were sealed with gasketed stainless steel lids with holes for gas exchange (Wako USA). Following cell attachment, library compounds were transferred by pintool (Wako USA) using 10 nl slotted pins. Library compounds were serially diluted in DMSO, and were added to plates to yield final concentrations of 0 (DMSO only), 4 and 20 μM compound. Following a 72 hour incubation at 37°C, cells were fixed, washed and stained similar to the 96-well OPC assay protocol, though all aspiration steps were performed using a Biotek EL406 Microplate Washer Dispenser (Biotek) equipped with a 1536-well aspiration manifold. Dispense steps were performed with both peristaltic pump cassettes (for gentle reagent additions) and syringe pump manifolds (for faster bulk dispenses). Cells were stained with DAPI (Sigma; 1μg/ml) and MBP antibody (Abcam, ab7349; 1:100). Plates were then imaged using an InCell 2000 Analyzer High Content Imager (GE Healthcare Bio-Sciences). Well images were analyzed using InCell Analyzer Workstation software, and MBP signal was quantified with a process detection algorithm, using total process skeleton length to qualify activity.

ex vivo cerebellar slice cultures

Whole cerebellum was harvested from postnatal day seven C57BL/6 mice and embedded in agarose. Sagittal slices were cut on a microtome (Leica) at 300 μm. Slices were cultured in a DMEM- Basal Medium Eagle's base with 15% heat-inactivated horse serum, modified N2 and PDGF-AA. After one day in culture, slices were treated daily for five days with test drugs or vehicle (DMSO). Drugs tested were: clobetasol (5 μM), hydroxyzine (5 μM), clotrimazole (2 μM), miconazole (1 μM), ketoconazole (1 μM), vesamicol (5 μM), propafenone (2 μM), dicyclomine (5 μM), benztropine (2 μM), haloperidol (5 μM), and medroxyprogesterone (5 μM). The identity of the drugs was blinded to the experimenter. Slices were then lysed for western blot or fixed in 4% PFA and processed for HCA as detailed below.

Immunohistochemistry

Immunohistochemistry was performed as previously described[3]. In short, tissue sections or whole slices were washed three times in PBS, blocked in PBS containing Triton X-100 (0.1%) and normal donkey serum (NDS, 2% for sections and 10% for cerebellar slices) and incubated with primary antibody overnight. For MBP immunohistochemistry the primary antibody solution consisted of 2% NDS, 2% bovine serum albumin, and 0.1% saponin. For all other antibodies the primary antibody solution consisted of 2% NDS and 0.1% Triton X-100. Primary antibodies used included rat anti-MBP (Abcam, ab7349; 1:100), mouse anti-APC CC1 clone (Millipore, MABC200; 1:500), and rabbit anti-IBA1 (Wako Chemicals, 019-19741; 1:1000). The tissue was then washed in PBS and incubated in secondary antibodies for two hours. Secondary detection was performed with Alexa Fluor-conjugated secondary antibodies (1:500) for one hour. Luxol fast blue staining was performed as previously described[7].

High content screen of cerebellar slices

MBP stained cerebellar slices were confocal imaged on the Operetta® system and analyzed using the PhenoLOGIC™ machine-learning technology within the Harmony® software. The software was trained to identify elongated fibers more characteristic of axonal ensheathment

and to exclude regions of small fibers or diffuse background fluorescence based on texture features. MBP positive surface area was collected and normalized to the total surface area for the group of slices treated with each drug. A minimum of six slices were treated per drug which included an equal distribution of medial and lateral slices.

Western blotting of cerebellar slices

Cerebellar slices (each biological replicate employing twelve slices per condition; six each from two separate animals) were collected in PBS and centrifuged. The PBS was aspirated and the pellet resuspended in 100 μL lysis buffer (20 mMTris, 137 mM NaCl, 5.0 mM EDTA pH=8.0, 10% glycerol, 1% NP40, pH to 8.0 with HCl), incubated on ice for 20 minutes, centrifuged and the supernatant collected. Protein concentration was determined by Pierce BCA protein assay kit (Thermo Fisher). Equal amounts of protein were applied to NuPAGE 12% Bis-TRIS gels (Life Technologies), and electrophoretically transferred onto a PVDF membrane (Life Technologies). The membranes were incubated with rabbit anti-MBP (Millipore, AB980; 1:500) and consequently probed with horseradish peroxidase-conjugated goat anti–rabbit (1:5,000) or incubated with HRP conjugated mouse anti-β-actin (Sigma, A3854; 1:10,000) to ensure even loading of samples. Enhanced chemiluminescence was performed with the West Pico kit (Thermo Fisher) and relative optical density analysis was measured using ImageJ (NIH).

Chemoinformatics

Structure-activity searches of azoles and steranes were performed with Canvas program (Schrodinger Software, Release 2014-1: Canvas, version 1.9). Tanimoto similarity between voriconazole and miconazole was calculated by ROCS (OpenEye Scientific Software).

Pharmacokinetics

C57BL/6 adult female mice were dosed i.p. with miconazole (10 mg/kg or 40 mg/kg) or clobetasol (10 mg/kg). After one or six hours, 100 μl of plasma was collected then each animal was perfused with PBS. Brains were collected, weighed, and rinsed with PBS. 0.5 mL of water was added to the brain samples and homogenized. Plasma and brain samples were each diluted five-fold with blank rat plasma. 300 μL of internal standard solution was added to the samples, vortexed, and centrifuged. 5 μL of each sample was injected into an API-4000Qtrap mass spectrometer and quantified (Climax Labs).

Focal demyelination and drug treatment

Focal demyelination in the spinal cord was induced by the injection of 1% LPC solution. 10–12 week old C57BL/6 female mice were anesthetized using isoflurane and a T10 laminectomy was performed. 1μl of 1% LPC was infused into the dorsal column at a rate of 15 ml/hour. The animals were euthanized either at day eight or day twelve after the laminectomy (n= 6–9 per group). Animals that were euthanized at day eight received vehicle or drug daily by i.p. injection between days three and seven. Animals used in the day twelve experiments received vehicle or drug daily by i.p injection between days four and eleven. Drugs were dissolved in DMSO and then diluted with sterile saline for injection. Mice were deeply anesthetized using ketamine/xylazine rodent cocktail and then euthanized by

transcardial perfusion with 4% PFA for histological analysis or 4% PFA, 2% gluteraldehyde, and 0.1 M sodium cacodylate for electron microscopy. PFA fixed tissue was equilibrated in 30% sucrose, embedded in OCT and cryosectioned at 20 μm thickness and processed for CC1 and MBP immunohistochemistry. ImageJ was used to measure area of the lesion and CC1+ cells within the lesion were scored manually. For CC1 scoring, sections were taken from the center of each lesion to control for lesion variability.

Electron microscopy

Samples were processed as previously described[3,24]. In short, samples were osmicated, stained *en bloc* with uranyl acetate and embedded in EMbed 812, an Epon-812 substitute (EMS). 1 μm sections were cut and stained with toluidine blue and visualized on a light microscope (Leica DM5500B). Additional thin sections were cut, carbon-coated and imaged either on JEOL JEM-1200-EX electron microscope or a T12 electron microscope (FEI).

Developmental myelination

Mouse pups of strain CD1 were administered 2 mg/kg clobetasol, 10 mg/kg miconazole, or vehicle (DMSO in saline) by daily i.p. injections from postnatal day two to six. Some clobetasol treated animals exhibited sickness based on this treatment, with low body weight and some animals of the cohort died before end of treatment. On postnatal day seven the pups were anesthetized using ketamine and xylazine and euthanized by transcardial perfusion with 4% PFA. Tissue was fixed overnight in 4% PFA, equilibrated in 30% sucrose and embedded in OCT. 20 μm sections were cut and processed for CC1 and MBP immunohistochemistry. ImageJ was then used to count and measure area of the corpus callosum as well as measure the extent of the corpus callosum length covered by MBP+ processes. Eight coronal sections containing corpus callosum rostral to the hippocampus from at least three animals per group were used for these analyses. To quantitate extent of MBP in the corpus callosum, a line was drawn through the center of the corpus callosum from the lateral tip to the dorsal most extent of MBP expression in the corpus callosum. The length of this line was measured and then the dorsal most point of the line was extended to the dorsal tip of the corpus callosum and measured to yield the length of the lateral callosum. The two numbers were divided to get the MBP/CC proportion. A two-tailed t-test was used to compare drug to vehicle treated groups.

Muscarinic receptor antagonism

Miconazole, clobetasol, and benztropine (all at 1 μM in DMSO) were sent to Select Screen (Life Technologies) with identities coded. GeneBLAzer or Tango assays were performed to determine level of acetylcholine muscarinic receptor M1, M3, M5, (GeneBLAzer) M2 and M5 (Tango) antagonism.

Kinase Profiling

LanthaScreen, Z'-LYTE, and Adapta kinase assays were performed by Select Screen (Life Technologies). LanthaScreen Eu kinase assays were performed in Greiner low-volume 384-well plates. Assay buffer consisted of 50 mM HEPES pH 7.5, 0.01% BRIJ-35, 10 mM MgCl$_2$, 1 mM EGTA. Each well consisted of this mixture: 4.0 μl of 4 μM test drug in assay

buffer, 8 μl of 2× kinase/Eu antibody mixture, and 4 μl of 4× Alexa Fluor 647 tracer. Plates were incubated for 60 minutes at room temperature, then AlexaFluor 647 Emission (665 nm) and Europium Emission (615 nm) read on a fluorescent plate reader. Data was analyzed by generating the emission ratio (665 nm/615 nm) for each test point and normalizing 0% to control wells with no known inhibitor and 100% to control wells with highest concentration of known inhibitor.

Z'-LYTE assays were performed in Corning, low volume 384-well plates. Assay buffer consisted of 50 mM HEPES pH 7.5, 0.01% BRIJ-35, 10 mM $MgCl_2$, 1 mM EGTA. Each well consisted of this mixture: 2.5 μl 4× of 4 μM drug in assay buffer, 5 μl 2× peptide/kinase mixture, 2.5 μl 4× ATP solution. Plates were then incubated at room temperature for 60 minutes. Then 5 μl of a development reagent that contains a protease that selectively digests the non-phosphorylated peptide was added and the plates incubated for 60 minutes. Coumarin Emission (445 nm) and Fluorescein Emission (520 nm) were read on a fluorescent plate reader. Data was analyzed by normalizing out background fluorescence then generating the emission ratio (445 nm/520 nm) for each test point. Data were further normalized to 0% in control wells with no ATP and 100% in control wells with synthetically phosphorylated peptide of the same sequence.

Adapta assays were performed in Corning, low volume 384-well plates. Assay buffer consisted of 30 mM HEPES. Each well consisted of this mixture: 2.5 μl 4× of 4 μM drug in assay buffer, 2.5 μl 4× ATP solution, 5μl 2× substrate/kinase mixture. Plates were then incubated at room temperature for 60 minutes. Then 5 μl of a development reagent that contains europium-anti-ADP antibody and ADP tracer was added and the plate incubated for 60 minutes. AlexaFluor 647 Emission (665 nm) and Europium Emission (615 nm) were read on a fluorescent plate reader. Data was analyzed by generating the emission ratio (665 nm/615 nm) for each test point and normalizing 0% to control wells with no ATP in the kinase reaction and 100% to control wells with ADP. Raw data from all kinase assays can be found in Supplementary Table 2.

High content analysis of astrocyte induction

For the astrocyte experiments in Fig. 3c, experimental setup was identical to the PLP1-based primary validation screen except plates were stained for GFAP (DAKO, Z0334; 1:5,000). BMP4 (R&D Systems; 50ng/ml) and LIF (Millipore; 10^3 units/ml) were used as the positive control for astrocyte induction. Assay plates were imaged on the Operetta® High Content Imaging and Analysis system and a set of 14 20× fields captured. Columbus™ Data Management and Analysis System software (PerkinElmer) was used to quantify the percent of GFAP+ astrocytes in each well using a method similar to that developed for oligodendrocytes.

Global phosphoproteomics

Quantitative global phosphorylation studies were performed on OPCs across two different time points (one and five hours post treatment) with miconazole, clobetasol or DMSO treatment using a label-free Ultra-high Performance LC-MS/MS workflow without fractionation. Briefly, for each sample 30 million cells were lysed with 2% SDS solution

with protease and phosphatase inhibitor (Thermo Fisher) and detergent removal was performed on 200 μl of the cell lysate using the FASP cleaning procedure[25]. Each sample was digested by a two-step Lys-C/Trypsin proteolytic cleavage and subjected to phospho-enrichment using a commercially available TiO2 enrichment spin tips (Thermo Fisher). LC-MS/MS analysis was performed using a UPLC system (NanoAcquity, Waters) that was interfaced to Orbitrap ProVelos Elite MS system (Thermo Fisher). Fold change calculations were determined from peptide intensities for each drug versus DMSO at each time point. Phosphopeptides with greater than two-fold change were imported into Ingenuity Pathway Analysis (IPA) to elucidate signaling pathways perturbed with drug treatment.

RNA sequencing and analysis

Cells were lysed directly in 1 ml TRIzol (Invitrogen) and stored in −80°C. Once all samples were collected, samples were thawed on ice and separated with chloroform using Phase Lock Gel tubes (5 PRIME). RNA was isolated using the miRNeasy Plus Mini Kit (Qiagen) according to the manufacturer's protocol. 1 μg of each sample was then poly-A selected, fragmented, and library prepped using the TruSeq RNA Sample Prep Kit (Illumina) according to the manufacturer's protocol. Samples were indexed using TruSeq adapters. 100 base-pair paired end reads were generated for each sample on an Illumina HiSeq 2500 instrument at the Case Western Reserve University Genomics Core facility. Between 5 and 13 million reads were generated per sample for drug time course experiments. EpiSC RNAseq data was previously published (GEO accession GSE57403)[26]. EpiSCs, EpiSC OPCs, and *in vivo* OPCs were sequenced to depths of 51,271,458 reads, 61,072,460 reads, and 62,530,709 reads respectively. For *in vivo* isolated OPCs, CD140a+ cells were immunopanned from the CNS of postnatal day seven mouse pups as described previously[27]. Cells were then cultured for five days in identical culture conditions to EpiSC-derived OPCs prior to analysis.

Reference genome files were retrieved from Illumina iGenomes (http://cufflinks.cbcb.umd.edu/igenomes.html). Reads were aligned to the mm9 genome using Tophat v2.0.8 with default settings[28]. Expression values of known RefSeq genes were calculated in units of fragments per kilobase per million reads (FPKM) using Cufflinks v2.0.2[29]. Expression values were tabled in order to eliminate background signal by converting all values below 0.25 to 0, and subsequently adding 0.25 to all values. FPKMs were quantile normalized to correct for inter-sample variation. In order to identify genes whose expression was perturbed by drug treatments, duplicate samples of OPCs were treated with drug or vehicle for two, six or twelve hours. RNA sequencing data was tested for differential expression by comparing treatments to vehicle at each time point using Cuffdiff v2.0.2[30]. The collective list of changed genes for each drug was evaluated with Ingenuity Pathway Analysis (Application Build 261899, Content Version 18030641).

Western blotting of mouse OPCs

EpiSC-derived OPCs were seeded into poly-L-ornithine/laminin coated 6-well plates and allowed to attach for two hours in DMEM/F12 without additional factors. Cells were treated with indicated inhibitors or DMSO for one hour—SCH772984 (ChemieTek, 1 μM), SB590885 (Tocris, 10 nM), LY294002 (Tocris, 10 μM), and PD0325901 (Stemgent, 1 μM).

Cells were then stimulated with drug or FGF2 (R&D Systems; 20 ng/ml) for one hour and then lysed in 200 μL RIPA buffer [0.15 M NaCl, 0.05 M Tris, pH=8.0, 1 mM EDTA, 1% Triton X-100, 0.1% SDS, 10% glycerol, HALT protease and phosphatase inhibitor (Thermo Fisher) added just before use] and incubated on ice for 20 minutes. Lysates were centrifuged at 4°C and supernatant collected. Protein concentrations were determined by Pierce BCA protein assay kit (Thermo Fisher). Equal amounts of protein were resolved in a reduced manner on NuPAGE 4–12% Bis-Tris gels (Life Technologies) and transferred onto PVDF membranes (Life Technologies). Blots were blocked in either 5% BSA (phosphoprotein) or 5% milk (non-phoshpoprotein). Primary antibodies were all from the same vendor (Cell Signaling) and included phospho-Erk1/2 (4370S, clone D13.14.4E; 1:2,000), ERK1/2 (9107S, clone 3A7; 1:2,000), phospho-glucocorticoid receptor (4161S; 1:1,000), and glucocorticoid receptor (12041, clone D6H2L; 1:1,000) followed by incubation with horseradish peroxidase-conjugated secondary antibodies and chemiluminescent enhancement by West Pico substrate (Thermo Fisher).

Generation and screening of human OPCs

Human OPCs were generated from skin fibroblast-derived human iPSC line (CWRU43, Tesar Lab) and hESC lines H7 (NIH Human Embryonic Stem Cell Registry WA07; NIH Approval Number: NIHhESC-10-0061) and H9 (NIH Human Embryonic Stem Cell Registry WA09; NIH Approval Number: NIHhESC-10-0062) as previously described[21,22]. iPSC and hESC-derived OPCs were characterized by Sox10 (R&D Systems, AF2864; 1:100) staining, and then seeded in 96 well plates at 40,000 cells per well for drug testing. Cells were cultured with 1 μM miconazole, 5 μM clobetasol, or vehicle (DMSO) for 21 days, with fresh media changes with drug or vehicle every two days. Plates were fixed and stained with MBP (Abcam, ab7349; 1:100) then imaged on the Operetta system. Analysis was performed with slight modification to HCA Acapella® scripts utilized for mouse oligodendrocytes.

Naïve CD4$^+$ T cell assays

Naïve CD4$^+$ T cells (CD4$^+$ L-selectin^{hi} cells) were purified using AutoMacs Magnetic Bead cell separation technology (Miltenyi Biotech) from total lymph node cells isolated from unprimed mice with purity ranging from 98–99.9%. For *in vitro* activation, $5×10^5$ naïve CD4$^+$ T cells were activated in the presence of plate-bound anti-CD3 (1 μg/ml) plus Th1-(200 U/ml IL-2, 40 U/ml IL-12, 10 μg/ml anti-IL-4) or Th17-(10 ng/ml TGF-β1, 50 ng/ml IL-6, 1 μg/ml anti-IFN-γ, 1 μg/ml anti-IL-4, 1 μg/ml anti-IL-2) promoting conditions. On day four the cultured T cells were collected and the percentage of viable cytokine positive cells assessed via flow cytometry. The cells were stained with LIVE/DEAD® Fixable Violet Dead Cell Stain Kit, for 405 nm excitation (Life Technologies), anti-CD4-APC/Cy7 (clone RM4–5), anti-IFN-γ-PerCP/Cy5.5 (clone XMG1.2), and anti-IL-17-APC (clone eBio17B7) (eBioscience). Viable cells ($5×10^5$) were analyzed per individual sample using a BD Canto II cytometer (BD Biosciences), and the data were analyzed using FloJo Version 9.5.2 software (Tree Star, Inc).

ex vivo lymphocyte recall assays

Female SJL/J (Harlan Labs) or C57BL/6 mice were housed under SPF conditions. Six to seven week old female mice were immunized subcutaneously with 100 μl of an emulsion containing 200 μg of *M. tuberculosis* H37Ra (BD Biosciences; San Jose, CA) and 50 μg of $PLP_{139-151}$ (SJL/J) or MOG_{35-55} (C57BL/6) distributed over three sites on the flank. For *ex vivo* culture draining lymph nodes on day eight were collected and cells were activated in the presence of anti-CD3 (1 μg/ml) in the absence or presence of clobetasol, miconazole, or benztropine (10^{-9}-10^{-5} M). To assess total cellular proliferation, cultures were pulsed with tritiated thymidine (1 μCi) at 24 hours and cultures were harvested at 72 hours. In replicate wells, culture supernatants were harvested at 72 hours post culture, and the level of IFN-γ and IL-17 were assessed via Luminex assay (Millipore).

$PLP_{139-151}$-induced relapsing remitting EAE

Six to seven week old female SJL/J mice were induced with $PLP_{139-151}$ as for *ex vivo* recall assays. Mice were allowed to progress to disease onset at day 13 before being randomized into treatment groups (n = 10 mice per group). Mice were then monitored for paralysis and treated daily via i.p. injection with vehicle (DMSO in sterile saline), benztropine (10 mg/kg), clobetasol (2 mg/kg), or miconazole (10 mg/kg) beginning on day 13 and ending on day 29. This time period fully encompassed the acute phase of disease onset followed by remission and the primary disease relapse. Treatments were blinded to the experimenters performing the assays. Mice were followed for disease severity in a blinded fashion with disease scoring as: 0=no abnormality; 1=limp tail; 2=limp tail and hind limb weakness; 3=hind limb paralysis; 4=hind limb paralysis and forelimb weakness; and 5=moribund.

### MOG_{35-55} chronic progressive EAE model

EAE was induced by immunizing ten week old C57BL/6 female mice with 100 μl injection of MOG_{35-55}/complete Freund's adjuvant Emulsion (Hooke Laboratories). One hour after immunization, mice were given 100 ng of pertussis toxin by 100 μl i.p. injection. A second dose of pertussis toxin was administered the next day. EAE onset was monitored daily and scored using a clinical scale where 0=no abnormality; 1=limp tail; 2=limp tail and hind limb weakness; 3=hind limb paralysis; 4=hind limb paralysis and forelimb weakness; and 5=moribund. Mice that appeared moribund or exhibited forelimb paralysis were immediately euthanized and not used for the study. Once mice reached peak of disease (~day 15; clinical score = 3) they were randomized into treatment groups and drug or vehicle (DMSO in saline) was administered i.p. daily for ten days (n = 12–16 mice per group). Doses for each drug were: miconazole (10 mg/kg), clobetasol (2 mg/kg) and benztropine (10 mg/kg). At these doses no drugs showed any overt evidence of toxicity to any of the animals. Experimenters were blinded to the identity of the treatments and animals were scored daily. Cumulative disease scores for each animal were calculated during the treatment period and a two-tailed t-test was performed to compare drug- to vehicle-treated groups. The extent of recovery for each animal was calculated as the difference between the peak disease score and the score at the end of each experiment and a two-tailed t-test was used to compare each treatment to vehicle. External validation of MOG_{35-55} EAE experiments (n = 12 mice per group) were carried out at Hooke Labs with experimenters

blinded to the identity of the substances. FTY720 (fingolimod, 1 mg/kg), a known immunomodulatory drug, was used as a positive control during external validation of miconazole (10 mg/kg).
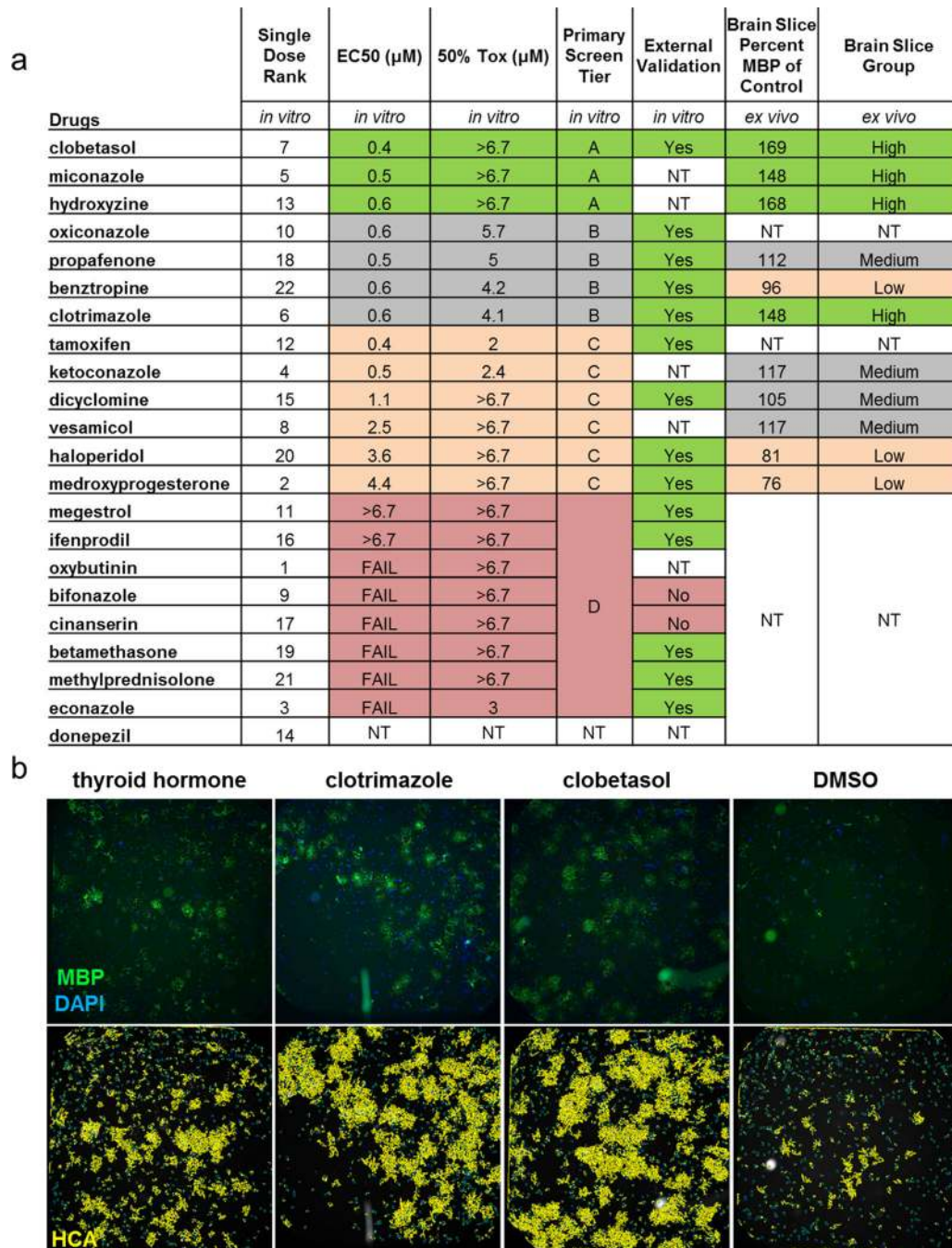
Animal welfare

All animal experiments were performed in accordance with protocols approved by the Case Western Reserve University and Northwestern University Institutional Animal Care and Use Committees (IACUC).

Extended Data
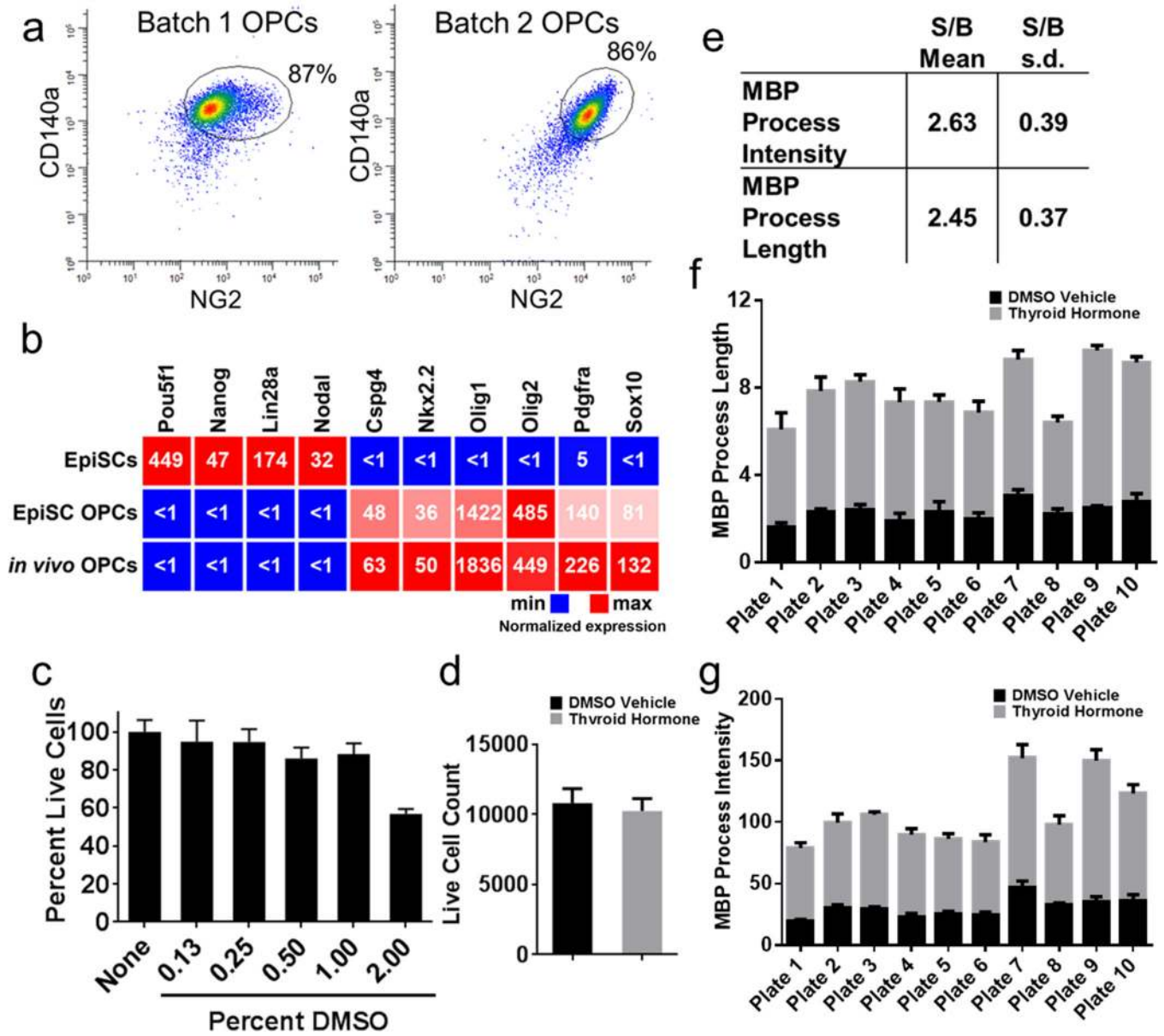
Extended Data Fig. 1. Performance of the primary screen

a, Representative flow cytometry plots showing co-expression of NG2 and CD140a in both batches of EpiSC-derived OPCs used for this study. The batches of EpiSC-derived OPCs were sorted to purity (circled areas of plots) prior to use in this study. **b**, RNAseq expression heatmap showing down regulation of pluripotent stem cell transcripts and up regulation of OPC transcripts when EpiSCs were differentiated into OPCs. Fragments per kilobase exon per million reads (FPKM) for each transcript are shown as compared to *in vivo* isolated mouse OPCs. **c**, Quantification of DMSO (v/v) tolerance of EpiSC derived-OPCs in 96-well plates shown as mean ± SEM. For reference, 0.05% (v/v) DMSO was used as vehicle for all *in vitro* experiments in this study. n = 16 wells per group with >690 cells scored per well. **d**, Quantification of cell viability of thyroid hormone (positive control) and DMSO vehicle treatments per well across all 10 assay plates shown as mean ± SEM. n = 80 wells per group with >6,800 cells scored per well. **e**, Signal to background (S/B) mean values with standard deviation (s.d.) of controls from the entire screen. n = 80 wells per group. **f**, Raw data of MBP process length from the primary screen for thyroid hormone treatment and DMSO vehicle across all plates shown as mean ± SD. n = 8 wells per group with >6,800 cells scored per well. **g**, Raw data of MBP process intensity from the primary screen for thyroid hormone treatment and DMSO vehicle shown as mean ± SD. n = 8 wells per group with >6,800 cells scored per well.
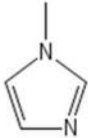
a

Drugs	Single Dose Rank	EC50 (µM)	50% Tox (µM)	Primary Screen Tier	External Validation	Brain Slice Percent MBP of Control	Brain Slice Group
	in vitro	in vitro	in vitro	in vitro	in vitro	ex vivo	ex vivo
clobetasol	7	0.4	>6.7	A	Yes	169	High
miconazole	5	0.5	>6.7	A	NT	148	High
hydroxyzine	13	0.6	>6.7	A	NT	168	High
oxiconazole	10	0.6	5.7	B	Yes	NT	NT
propafenone	18	0.5	5	B	Yes	112	Medium
benztropine	22	0.6	4.2	B	Yes	96	Low
clotrimazole	6	0.6	4.1	B	Yes	148	High
tamoxifen	12	0.4	2	C	Yes	NT	NT
ketoconazole	4	0.5	2.4	C	NT	117	Medium
dicyclomine	15	1.1	>6.7	C	Yes	105	Medium
vesamicol	8	2.5	>6.7	C	NT	117	Medium
haloperidol	20	3.6	>6.7	C	Yes	81	Low
medroxyprogesterone	2	4.4	>6.7	C	Yes	76	Low
megestrol	11	>6.7	>6.7	D	Yes	NT	NT
ifenprodil	16	>6.7	>6.7	D	Yes		
oxybutinin	1	FAIL	>6.7	D	NT		
bifonazole	9	FAIL	>6.7	D	No		
cinanserin	17	FAIL	>6.7	D	No		
betamethasone	19	FAIL	>6.7	D	Yes		
methylprednisolone	21	FAIL	>6.7	D	Yes		
econazole	3	FAIL	3	D	Yes		
donepezil	14	NT	NT	NT	NT		

b

thyroid hormone   clotrimazole   clobetasol   DMSO

MBP
DAPI

HCA

Extended Data Fig. 2. Drug hit ranking and validation

a, Chart ranking the 22 primary drug hits (Single Dose Rank) into 4 tiers based on calculation of half maximal effective concentration (EC_{50}) to induce PLP1+ oligodendrocytes from OPCs and concentration at which 50% of the cells were lost (50% Tox) calculated from a seven-point dose treatment. n = 4 wells per dose per drug using independently sourced drug and separate OPC batch from the primary screen. Tiers ranged from the most potent and least toxic effectors to the least potent and most toxic: Tier A (green), Tier B (grey), Tier C (orange) and Tier D (red). 1536-well format external
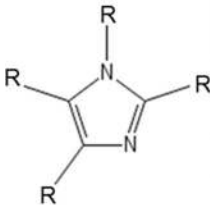
validation of 14 of 16 tested hits is also shown. Drugs were further ranked into groups of High (green), Medium (grey), and Low (orange) based on their ability to increase MBP+ axonal ensheathment in mouse cerebellar brain slices relative to vehicle (DMSO) treated controls as measured by HCA. NT = not tested. **b**, External validation whole 1536-well images of MBP+ (green) oligodendrocytes generated from OPCs after 72 hours of treatment. GE InCell HCA is shown with processes traced in yellow and nuclei in blue.

a
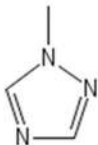
(1,3) Diazoles, mono-substituted at the 1-position	Primary Screen Rank
econazole	3
ketoconazole	4
miconazole	5
clotrimazole	6
bifonazole	9
oxiconazole	10
ozagrel	428
1-benzylimidazole	616

b

(1,3) Diazoles, poly-substituted	Primary Screen Rank
telithromycin	27
metronidazole	60
ondansetron	116
azathioprine	315
(+)-etomidate	322
ornidazole	327
pilocarpine	473
methimazole	483
tinidazole	589
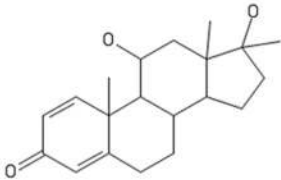
c

(1,2,4) Triazoles, mono-substituted at the 1-position	Primary Screen Rank
rizatriptan	214
voriconazole	219
letrozole	271
itraconazole	413
fluconazole	414
anastrazole	571

d

| Steroids	Primary Screen Rank
clobetasol	7
betamethasone	19
methylprednisolone	21
budesonide	28
triamcinolone	29
amcinonide	35
fluticasone	37
fluorometholone	38
depo-medrol	41
beclomethasone	44
loteprednol	45
fluocinolone	47
dexamethasone	49
hydrocortisone	50
halometasone	52
flucinonide	57
prednisolone	67
desoximetasone	100
dehydrocholic Acid	188
mestanolone	198
exemestane	212
flunisolide	259
prednisone	528

Extended Data Fig. 3. Primary screen structure-activity analysis

Chemoinformatic identification of two substructures consistently enriched in high performing drugs in the OPC assay. Numerical activity rank in the primary screen is indicated with the top 22 shown in green, 23–50 shown in grey, and >51 in red. **a**, (1,3) diazoles, mono-substituted at the 1-position showed consistent activity on OPCs. **b, c**, (1,3) diazoles, poly-substituted at 2 or more of the R groups (**b**), or (1,2,4) triazoles, mono-substituted at the 1-position (**c**) showed no activity on OPCs. **d**, The sterane base structure showed enrichment in the top performing hits.
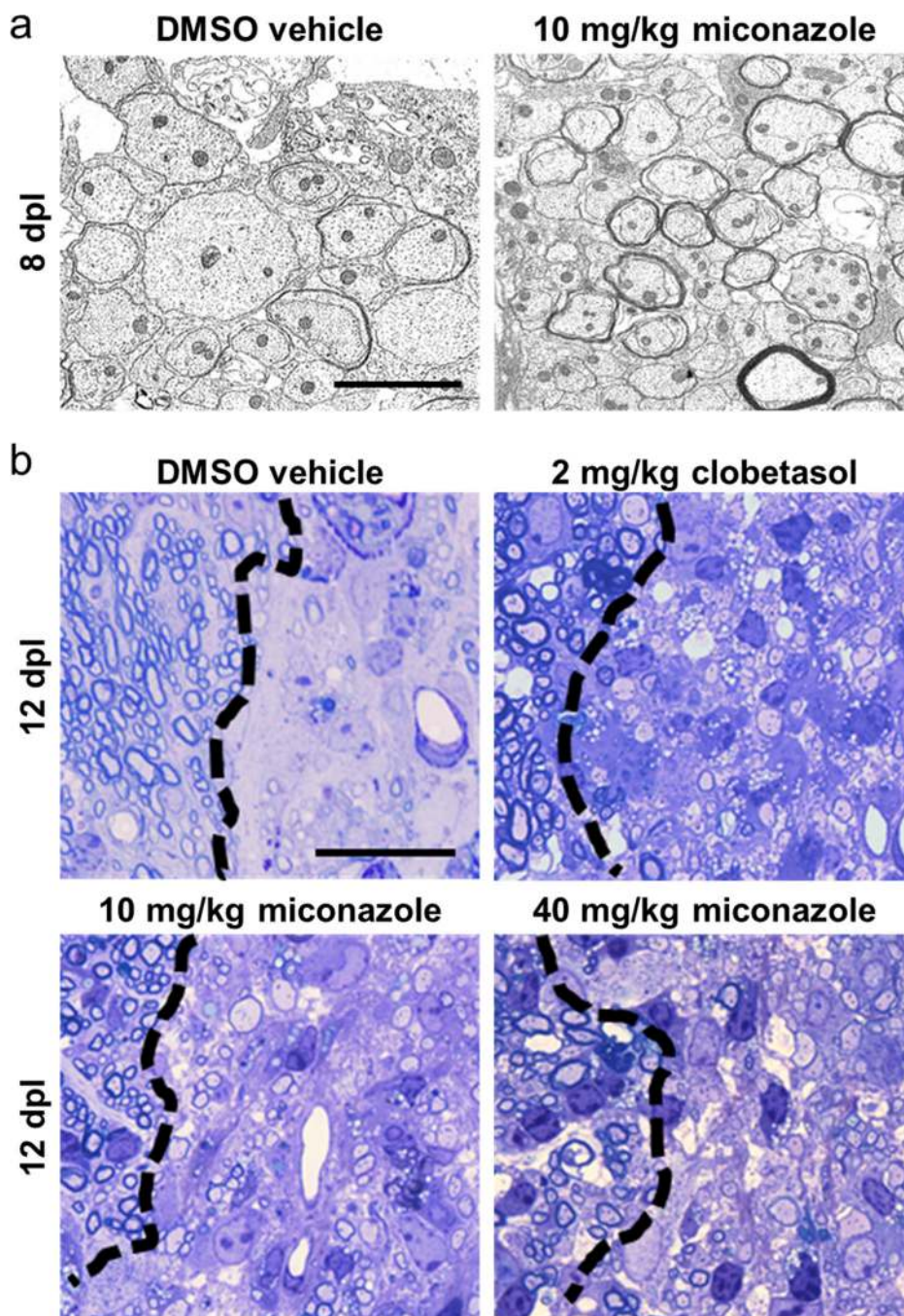
Extended Data Fig. 4. Histological assessment of remyelination in the LPC-induced model of demyelination
a, Representative electron micrographs showing remyelinated axons within lesions of miconazole treated mice at eight dpl. Scale bar, 2 μm. **b**, Toluidine blue stained histological sections showing the extent of remyelination in the lesions of treated animals at twelve dpl. Normal uninjured myelin appears to the left of the black dashed line demarcating the definitive lesion edge. Scale bar, 20 μm.
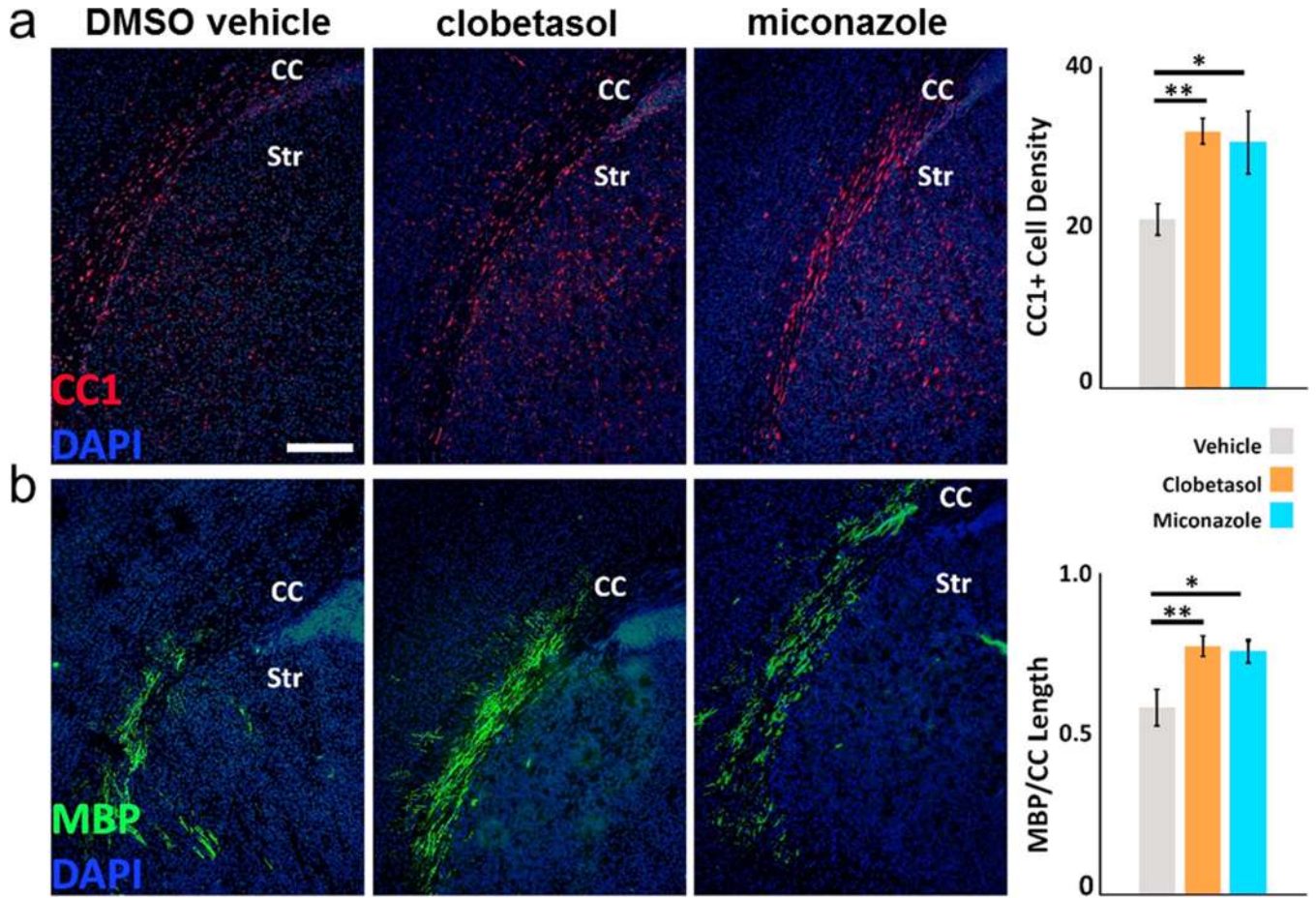
Extended Data Fig. 5. Miconazole and clobetasol enhance myelination *in vivo*
a and **b**, Representative immunohistochemical images of the lateral corpus callosum (CC) of postnatal day day mouse pups that had been injected i.p. daily for four days previously starting on postnatal day two with vehicle, clobetasol (2 mg/kg), or miconazole (10 mg/kg). CC1 (red) marks newly generated oligodendrocytes (**a**) and MBP (green) shows the extent of developmental myelination (**b**). Clobetasol and miconazole treatment each induce a marked increase in the number of CC1 positive oligodendrocytes in the lateral corpus callosum (**a**) and a significant increase in the length of the corpus callosum covered with aligned MBP+ fibers (**b**). Scale bar, 200 μm. Two-tailed t-test *p ≤0.05 and **p ≤0.01. Striatum is marked as Str. All graphs are presented as mean ± SEM.
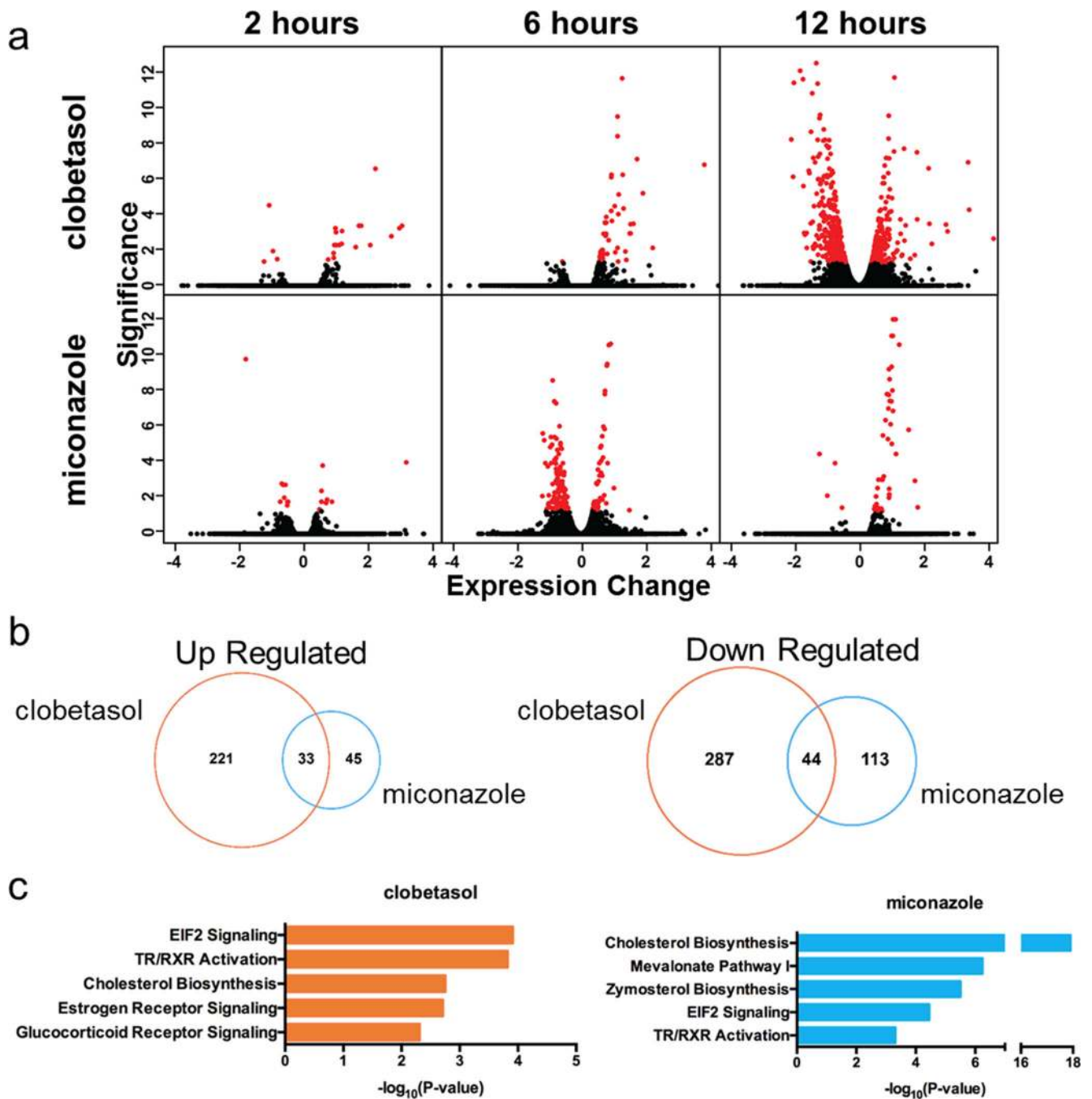
**Extended Data Fig. 6. RNAseq time course of drug treated OPCs**

a, Volcano plots of all genes from OPCs treated with clobetasol or miconazole relative to vehicle control, with differentially expressed genes highlighted (red). Significance (measured as $-\log_{10}$[q-value]) is plotted in relationship to expression change ($\log_2$[treatment/vehicle]). Time course was after two, six and twelve hours of drug treatment. **b**, Venn diagrams depicting the overlap of genes differentially expressed at any time point and increased in treatments vs vehicle (left), as well as those decreased in

treatments vs vehicle (right). **c**, Significant canonical pathways perturbed by each drug treatment according to Ingenuity Pathway Analysis.

Extended Data Fig. 7. Global phosphoproteomic analysis of miconazole-treated OPCs
a and **b**, OPCs treated with miconazole for one (**a**) or five (**b**) hours followed by global phosphoproteomic analysis. Proteins highlighted in green were observed to have a two-fold or greater increase in phosphorylation while those highlighted in red were observed to have a two-fold or greater decrease in phosphorylation as compared to time point matched vehicle

treated controls. Proteins highlighted in grey were detected in the analysis but were not changed compared to vehicle control. See Supplementary Table 3 for the full phosphoproteomic dataset. **c**, Quantification of the percentage of MBP+ oligodendrocytes differentiated from mouse OPCs after 72 hours of treatment with DMSO, miconazole (1 μM), or voriconazole (7 doses 0.01–6.7 μM). n = 6 wells per condition with >6,000 cells scored per well. Graph presented as mean ± SEM. The chemical structure of voriconazole is shown.
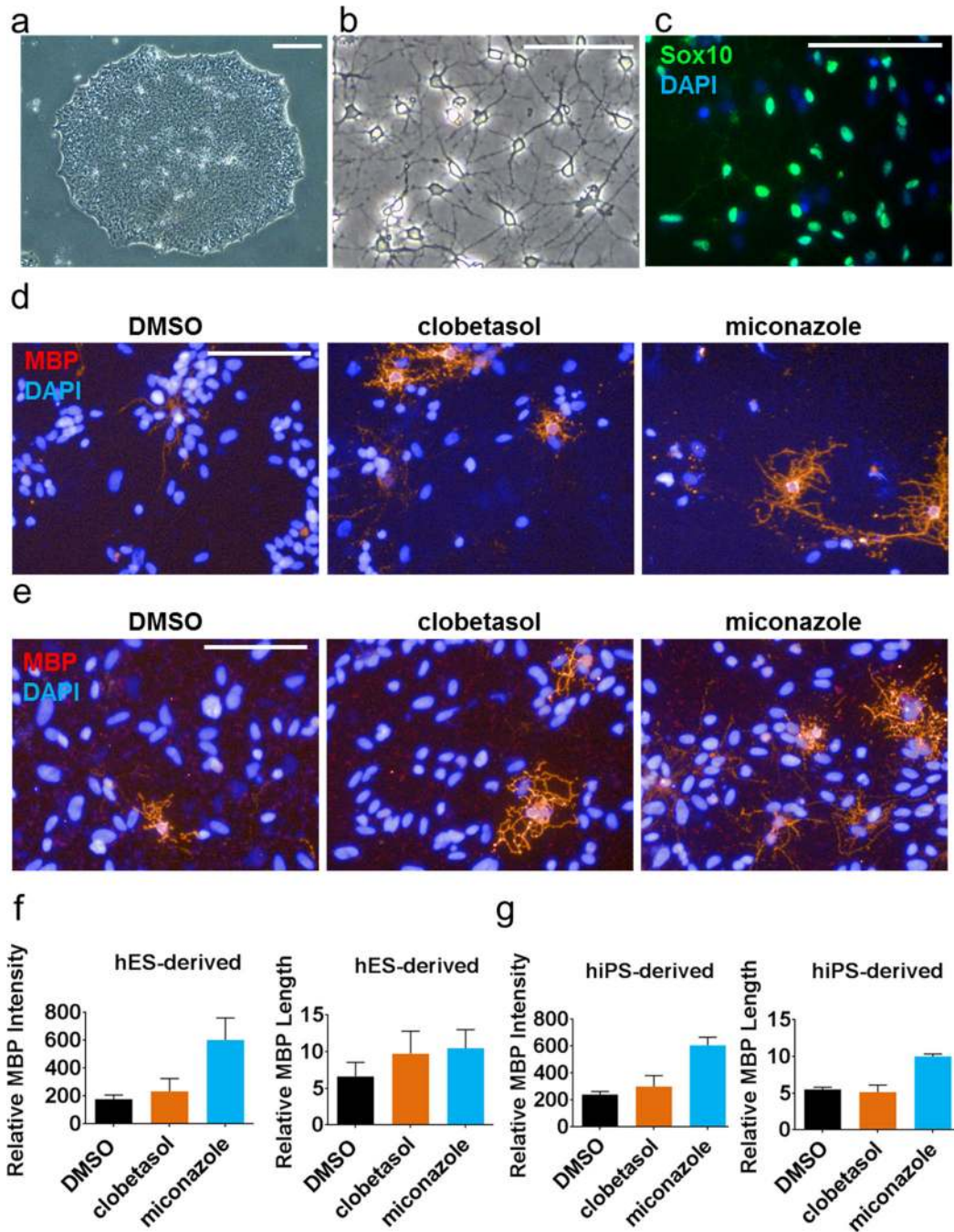
Extended Data Fig. 8. Miconazole and clobetasol enhance human OPC differentiation
a, Representative phase contrast image of a hESC colony cultured on matrigel. **b**, Representative phase contrast image of hESC-derived OPCs. **c**, hESC-derived OPCs stain positive for Sox10. **d** and **e**, Representative images of hESC-derived OPCs (**d**) and hiPSC-derived OPCs (**e**) treated with vehicle (DMSO), miconazole (1 μM), or clobetasol (5 μM) for 21 days stained for MBP (red). **f** and **g**, High content analysis of hESC-derived (**f**) and hiPSC-derived (**g**) OPCs differentiated in the presence of drugs or vehicle over 21 days. n = 3–5 wells per condition with >120 cells scored per well. Graphs presented as mean ± SEM. Scale bars, 100μm.
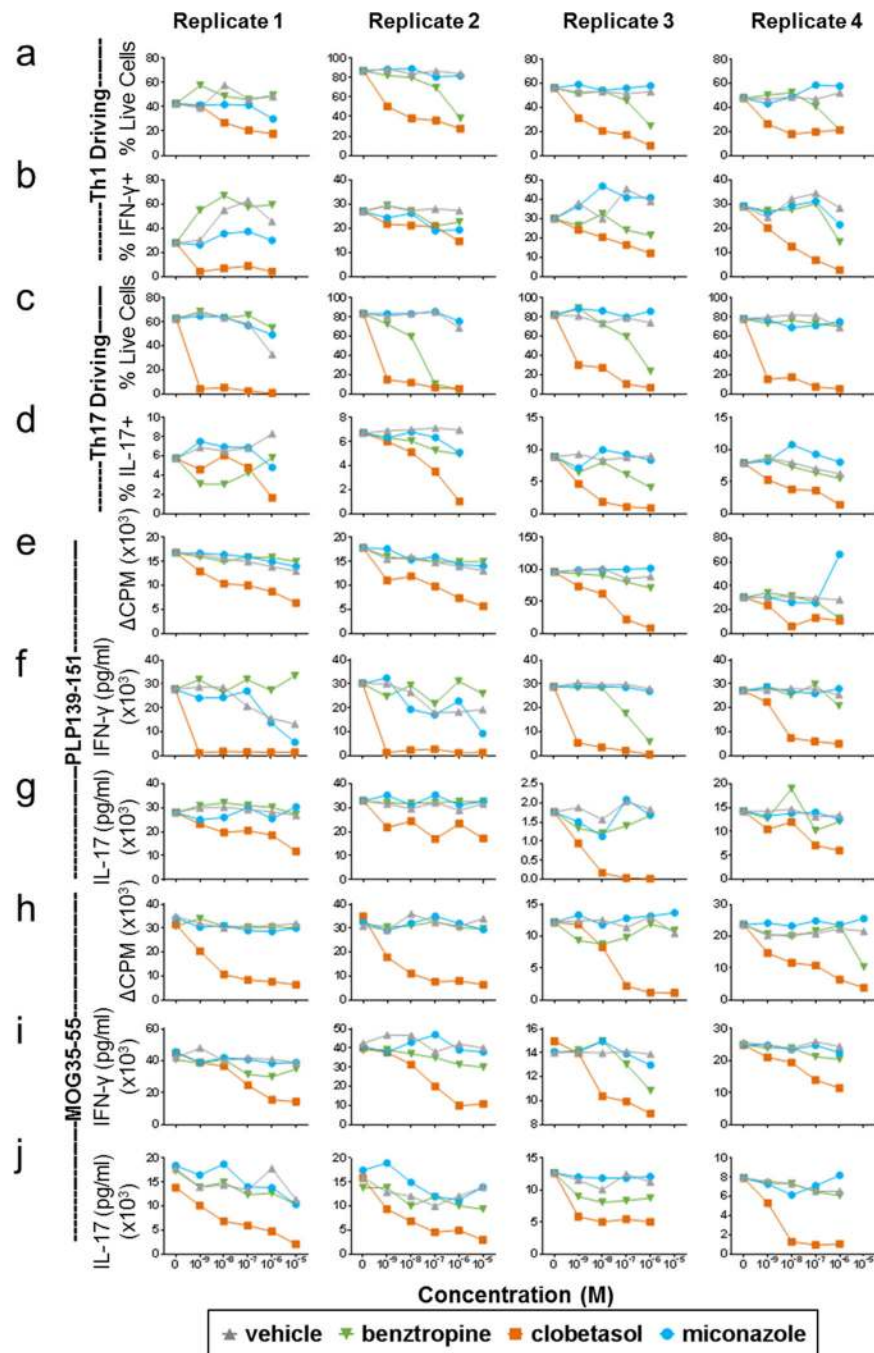
Extended Data Fig. 9. Effects of miconazole and clobetasol on immune cell survival and function
a–d, Quantification of cell proliferation (**a, c**) and differentiation (**b, d**) of naïve CD4+ T cells from unprimed SJL/J mice after activation with plate-bound anti-CD3 under Th1 (**a, b**) or Th17 (**c, d**) cell driving conditions. **e–j**, Ex vivo recall assays quantifying cell proliferation (ΔCPM) (**e, h**) along with interferon gamma (IFN-γ) (**f, i**) and IL-17 (**g, j**) cytokine production from lymphocytes of mice primed with PLP$_{139–151}$ (**e–g**) or MOG$_{35–55}$ (**h–j**). Cultures were treated with vehicle (DMSO), benztropine, clobetasol, or miconazole

$(10^{-9}\text{-}10^{-5}$ M) and analyzed after four days. Four independent replicates are shown for each assay.
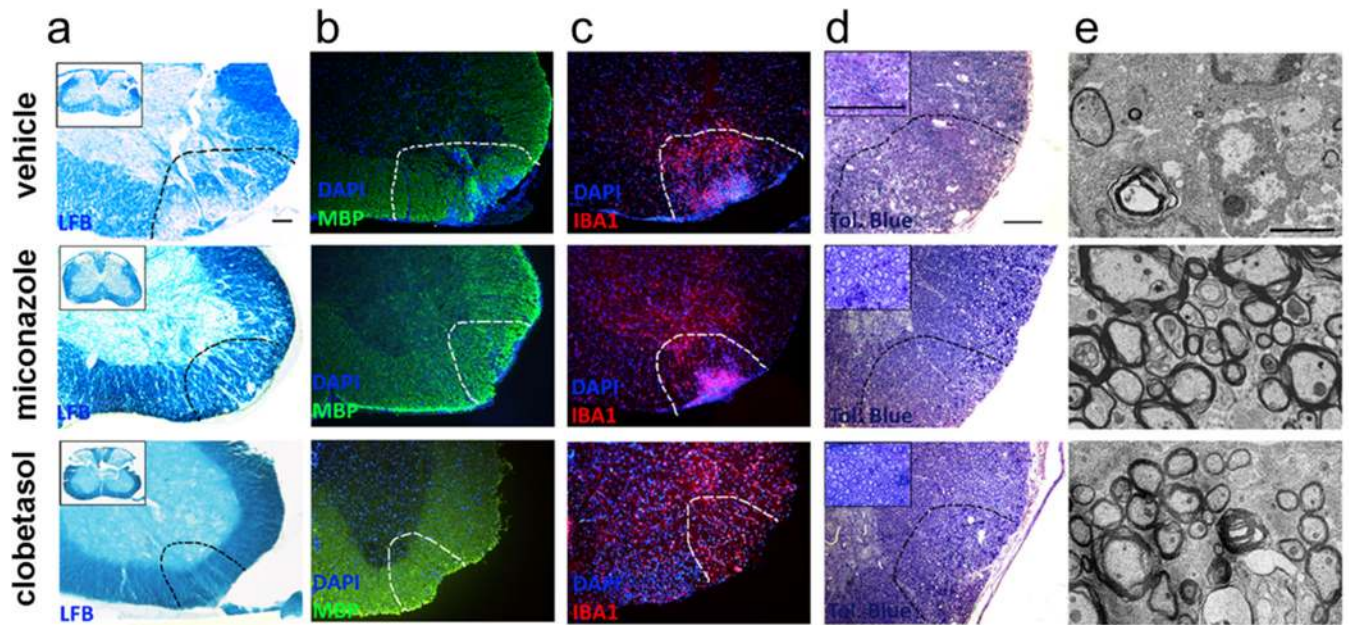
Extended Data Fig. 10. Histological improvements in MOG$_{35-55}$ EAE spinal cords after treatment with miconazole or clobetasol
a, b Representative images of luxol fast blue (LFB) staining (**a**) demonstrated a clear decrease in areas of white matter disruption in the spinal cords of drug treated animals which coincides with increased MBP staining (**b**). **c**, IBA1 staining showed a small reduction of immune cell infiltration into the lesion areas, especially in clobetasol treated animals, but not an abrogation, **d** and **e**, Representative toluidine blue stained images (**d**) and electron micrographs (**e**) revealed a reduction in the areas of demyelination in drug treated animals. Lesioned areas are outlined with black dotted lines. Insets in toluidine blue staining show higher magnification of myelination in the corresponding spinal cords. Scale bar, 100 μm (**a–d**) and 2 μm (**e**).

Supplementary Material

Refer to Web version on PubMed Central for supplementary material.

Acknowledgements

REFERENCES

1. Goldman SA, Nedergaard M, Windrem MS. Glial progenitor cell-based treatment and modeling of neurological disease. Science. 2012; 338:491–495. [PubMed: 23112326]

2. Chang A, Tourtellotte WW, Rudick R, Trapp BD. Premyelinating oligodendrocytes in chronic lesions of multiple sclerosis. N Engl J Med. 2002; 346:165–173. [PubMed: 11796850]

3. Najm FJ, et al. Rapid and robust generation of functional oligodendrocyte progenitor cells from epiblast stem cells. Nature Methods. 2011; 8:957–962. [PubMed: 21946668]

4. Tesar PJ, et al. New cell lines from mouse epiblast share defining features with human embryonic stem cells. Nature. 2007; 448:196–199. [PubMed: 17597760]

5. Brons IG, et al. Derivation of pluripotent epiblast stem cells from mammalian embryos. Nature. 2007; 448:191–195. [PubMed: 17597762]

6. Mi S, et al. Promotion of central nervous system remyelination by induced differentiation of oligodendrocyte precursor cells. Ann Neurol. 2009; 65:304–315. [PubMed: 19334062]

7. Bai L, et al. Hepatocyte growth factor mediates mesenchymal stem cell-induced recovery in multiple sclerosis models. Nat Neurosci. 2012; 15:862–870. [PubMed: 22610068]

8. Deshmukh VA, et al. A regenerative approach to the treatment of multiple sclerosis. Nature. 2013; 502:327–332. [PubMed: 24107995]

9. Mei F, et al. Micropillar arrays as a high-throughput screening platform for therapeutics in multiple sclerosis. Nat Med. 2014; 20:954–960. [PubMed: 24997607]

10. Fancy SP, et al. Overcoming remyelination failure in multiple sclerosis and other myelin disorders. Exp Neurol. 2010; 225:18–23. [PubMed: 20044992]

11. Franklin RJ, Ffrench-Constant C. Remyelination in the CNS: from biology to therapy. Nature Reviews. Neuroscience. 2008; 9:839–855. [PubMed: 18931697]

12. Dubois-Dalcq M, Ffrench-Constant C, Franklin RJ. Enhancing central nervous system remyelination in multiple sclerosis. Neuron. 2005; 48:9–12. [PubMed: 16202704]

13. Barres BA, Lazar MA, Raff MC. A novel role for thyroid hormone, glucocorticoids and retinoic acid in timing oligodendrocyte development. Development. 1994; 120:1097–1108. [PubMed: 8026323]

14. Woodruff RH, Franklin RJ. The expression of myelin basic protein exon 1 and exon 2 containing transcripts during myelination of the neonatal rat spinal cord--an in situ hybridization study. J Neurocytol. 1998; 27:683–693. [PubMed: 10447242]

15. Woodruff RH, Franklin RJ. The expression of myelin protein mRNAs during remyelination of lysolecithin-induced demyelination. Neuropathol Appl Neurobiol. 1999; 25:226–235. [PubMed: 10417664]

16. Jeffery ND, Blakemore WF. Remyelination of mouse spinal cord axons demyelinated by local injection of lysolecithin. J Neurocytol. 1995; 24:775–781. [PubMed: 8586997]

17. Kumar S, Cole R, Chiappelli F, de Vellis J. Differential regulation of oligodendrocyte markers by glucocorticoids: post-transcriptional regulation of both proteolipid protein and myelin basic protein and transcriptional regulation of glycerol phosphate dehydrogenase. Proc Natl Acad Sci U S A. 1989; 86:6807–6811. [PubMed: 2475873]

18. Morisaki S, et al. Endogenous glucocorticoids improve myelination via Schwann cells after peripheral nerve injury: An in vivo study using a crush injury model. Glia. 2010; 58:954–963. [PubMed: 20169622]

19. Ishii A, Fyffe-Maricich SL, Furusho M, Miller RH, Bansal R. ERK1/ERK2 MAPK signaling is required to increase myelin thickness independent of oligodendrocyte differentiation and initiation of myelination. J Neurosci. 2012; 32:8855–8864. [PubMed: 22745486]

20. Fyffe-Maricich SL, Schott A, Karl M, Krasno J, Miller RH. Signaling through ERK1/2 controls myelin thickness during myelin repair in the adult central nervous system. J Neurosci. 2013; 33:18402–18408. [PubMed: 24259565]

21. Hu BY, Du ZW, Zhang SC. Differentiation of human oligodendrocytes from pluripotent stem cells. Nat Protoc. 2009; 4:1614–1622. [PubMed: 19834476]

22. Wang S, et al. Human iPSC-derived oligodendrocyte progenitor cells can myelinate and rescue a mouse model of congenital hypomyelination. Cell Stem Cell. 2013; 12:252–264. [PubMed: 23395447]

REFERENCES FOR ONLINE METHODS

23. Najm FJ, et al. Isolation of epiblast stem cells from preimplantation mouse embryos. Cell Stem Cell. 2011; 8:318–325. [PubMed: 21362571]

24. Najm FJ, et al. Transcription factor-mediated reprogramming of fibroblasts to expandable, myelinogenic oligodendrocyte progenitor cells. Nature Biotechnology. 2013; 31:426–433.

25. Wisniewski JR, Nagaraj N, Zougman A, Gnad F, Mann M. Brain phosphoproteome obtained by a FASP-based method reveals plasma membrane protein topology. J Proteome Res. 2010; 9:3280–3289. [PubMed: 20415495]

26. Factor DC, et al. Epigenomic comparison reveals activation of "seed" enhancers during transition from naive to primed pluripotency. Cell Stem Cell. 2014; 14:854–863. [PubMed: 24905169]

27. Cahoy JD, et al. A transcriptome database for astrocytes, neurons, and oligodendrocytes: a new resource for understanding brain development and function. J Neurosci. 2008; 28:264–278. [PubMed: 18171944]

28. Trapnell C, Pachter L, Salzberg SL. TopHat: discovering splice junctions with RNA-Seq. Bioinformatics. 2009; 25:1105–1111. [PubMed: 19289445]

29. Trapnell C, et al. Transcript assembly and quantification by RNA-Seq reveals unannotated transcripts and isoform switching during cell differentiation. Nature Biotechnology. 2010; 28:511–515.

30. Trapnell C, et al. Differential analysis of gene regulation at transcript resolution with RNA-seq. Nature Biotechnology. 2013; 31:46–53.
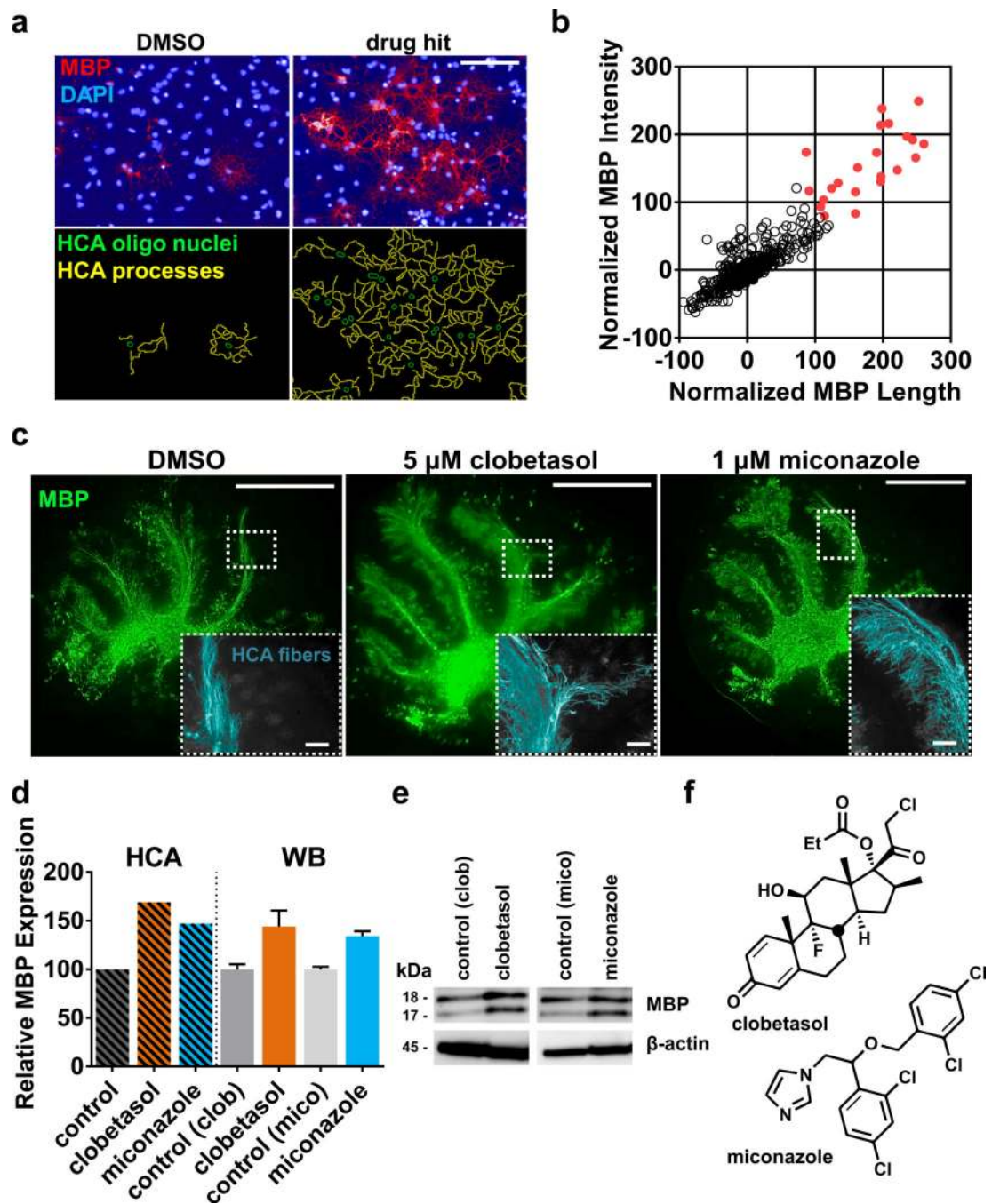
Figure 1. A pluripotent stem cell-based phenotypic screening platform to identify modulators of OPC differentiation and maturation

a, Representative images of vehicle and drug hit treated mouse EpiSC-derived OPCs from the primary screen. Nuclear (DAPI, blue) and MBP (red) staining along with high content analysis (HCA) to identify oligodendrocyte nuclei (green) and MBP+ processes (yellow). Scale bar, 100μm. **b**, Scatter plot of primary screen results displayed as normalized values of MBP process length and intensity for all 727 drugs with the 22 hits marked in red. Baseline (vehicle) was set at zero and thyroid hormone (positive control) was set at 100. **c**, Montaged

images of whole postnatal day seven mouse cerebellar slices treated with drug or vehicle for five days and stained for MBP (green). Insets show a representative example of the HCA script used to identify and quantify MBP+ aligned fibers (light blue). Scale bar, 1 mm for whole slices and 100 μm for insets. **d**, Relative quantitation of HCA and western blot (WB) data from cerebellar slices treated for five days. For HCA screen, n = 1 with 6–12 slices averaged per group (also see Extended Data Fig. 2a). For western blot, n = 3 independent replicates of 12 slices per group. Values are mean for HCA and mean ± SEM for WB. **e**, Representative WB of MBP isoforms and β-Actin (loading control) of cerebellar slices treated for five days. Full blots are available in Supplementary Figure 1. **f**, Chemical structures of clobetasol and miconazole. Source Data is provided for Figure 1b, d.
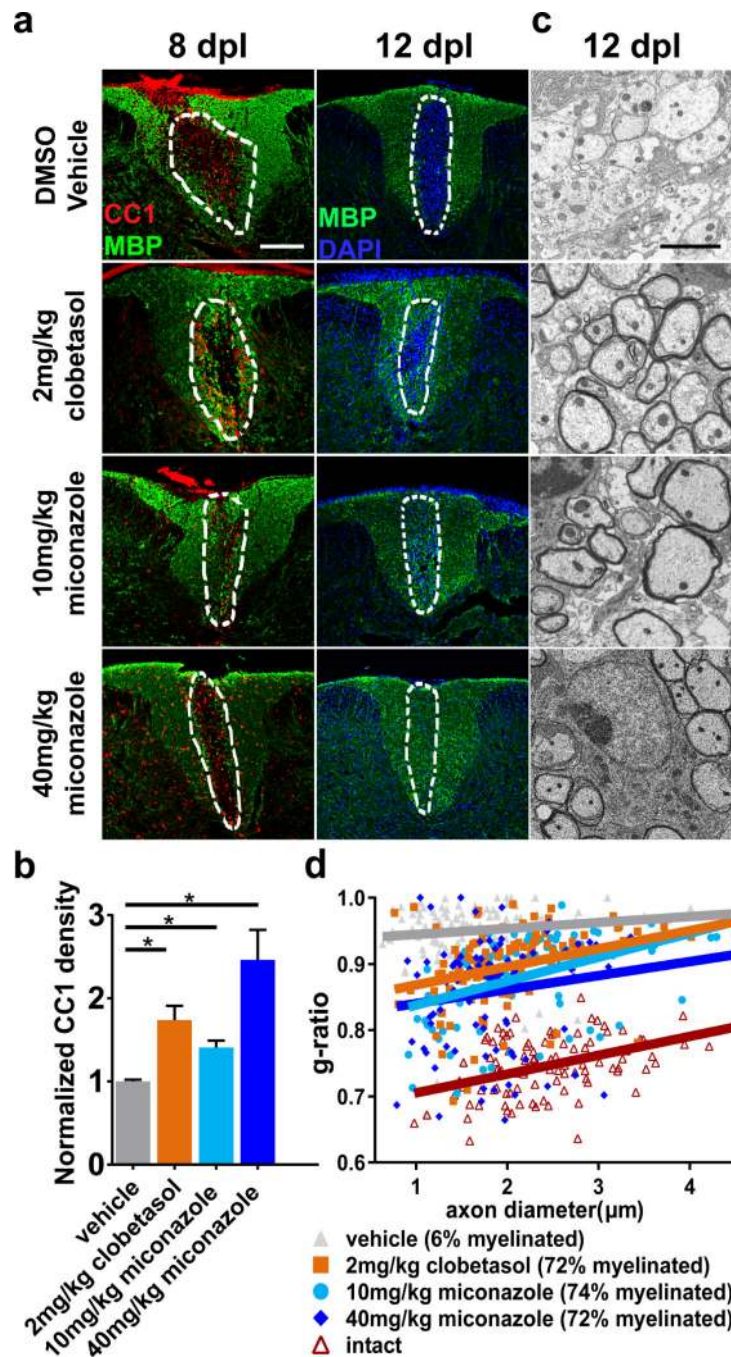
Figure 2. Miconazole and clobetasol each enhance remyelination in the LPC lesion mouse model
a, Representative immunohistochemical images of treated mice showing newly generated oligodendrocytes (CC1, red) and MBP (green) within the lesion (approximated by white dashed outline) at eight and twelve dpl. Scale bar, 200 μm. **b**, Quantitation of CC1+ oligodendrocytes per lesion area at eight dpl. Values are mean ± SEM. n = 3 mice per group. Two-tailed t-test *p<0.05. **c**, Representative electron micrographs showing remyelinated axons within lesions of drug treated mice at twelve dpl. Scale bar, 2 μm. **d**, Scatter plot of g-ratios of lesion axons at twelve dpl. n = 100 calculated from two mice per group. Percentage

of lesion axons myelinated is indicated in the legend. Source Data is provided for Figure 2b, d.
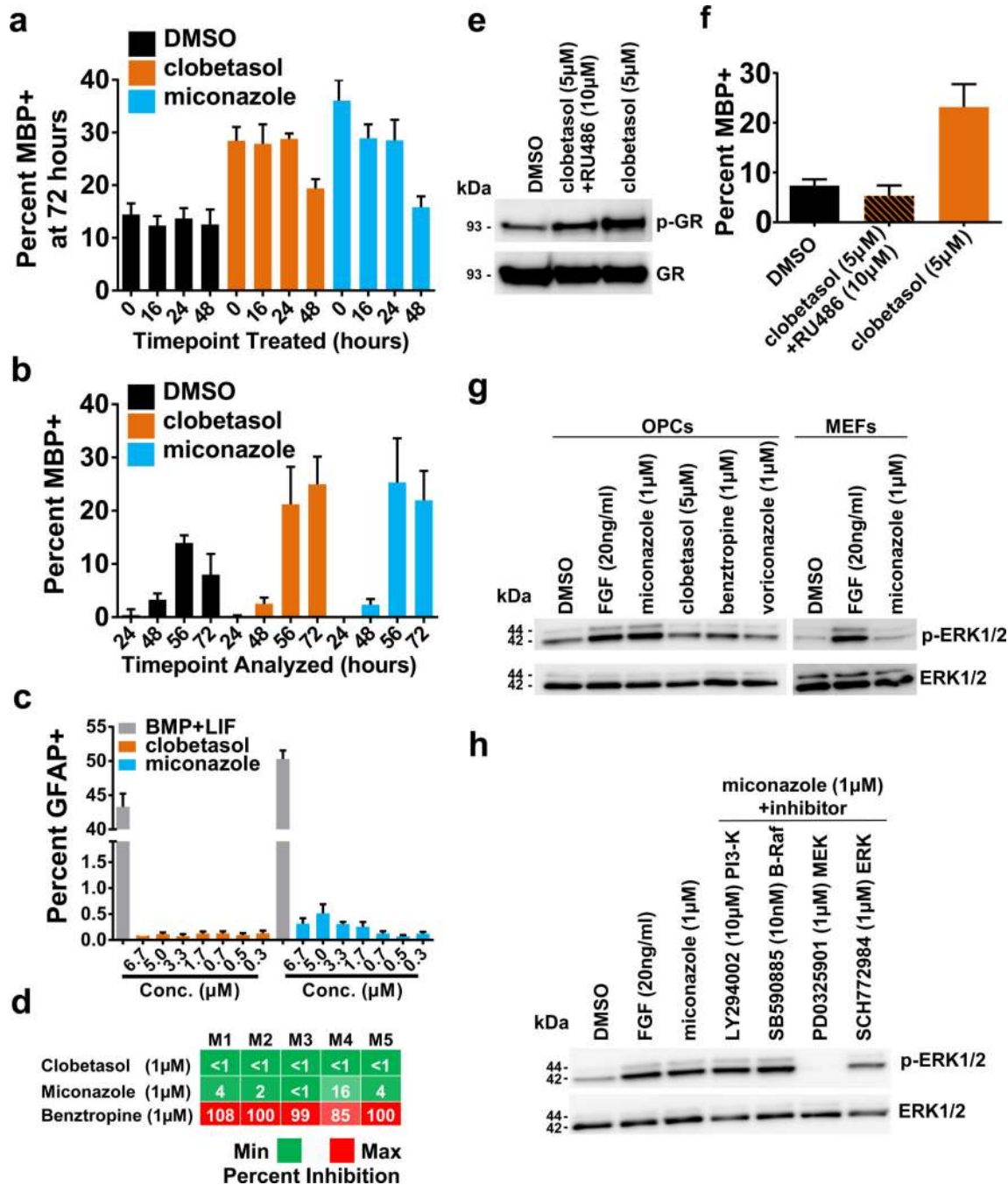
Figure 3. Cellular and molecular effects of miconazole and clobetasol on mouse OPCs
a, Percent MBP+ oligodendrocytes generated from OPCs at 72 hours with treatments initiated at time points indicated. n = 6 wells per condition with >6,000 cells scored per well. **b**, Percent MBP+ oligodendrocytes generated from OPCs treated simulataneously and analyzed at time points indicated. n = 8 wells per condition with >1,700 cells scored per well. **c**, Percent GFAP+ astrocytes generated from OPCs at 72 hours of treatment. n = 4 wells per condition >2,900 cells scored per well. **d**, Heatmap depicting biochemical inhibition of muscarinic receptors M1-M5 displayed as percent inhibition with minimum

(green) and maximum (red). **e**, Western blot of total GR and its phosphorylation at Ser220 (p-GR) in OPCs treated for one hour. **f**, Percent MBP+ oligodendrocytes generated from OPCs 72 hours after treatment. n = 6 wells per condition with >1,400 cells scored per well. **g**, Western blot of total ERK1/2 and their phosphorylation at Thr202/Tyr204 or Thr185/Tyr187 (p-ERK1/2) in cells (OPCs or mouse embryonic fibroblasts) treated for one hour. FGF served as a positive control for p-ERK1/2 induction. **h**, Western blot of total ERK1/2 and p-ERK1/2 in OPCs treated for one hour in the presence of the indicated pathway inhibitors. All graphs depict mean ± SEM. Full western blots are available in Supplementary Figure 2. Source Data is provided for Figure 3a–d, f.
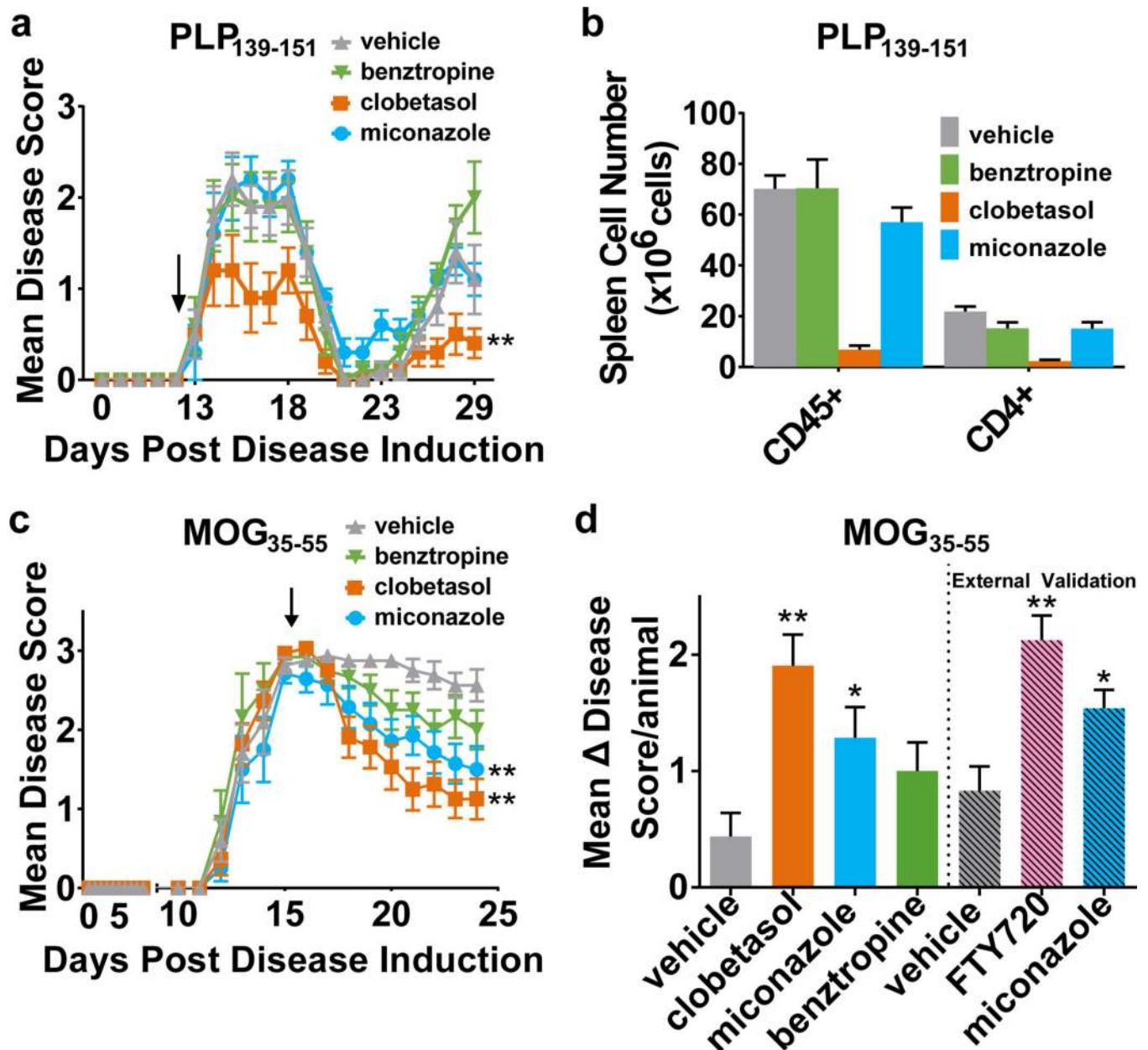
Figure 4. Therapeutic efficacy of miconazole and clobetasol in mouse models of multiple sclerosis
a, Scoring of disease severity in relapsing remitting PLP$_{139-151}$-induced EAE mice treated beginning on day 13 (black arrow) and ending on day 29. n = 10 mice per group. Graph depicts mean daily disease score ± SEM. **b**, Flow cytometric-based quantification of spleen cell numbers at day 29 from the PLP$_{139-151}$ EAE cohort in (**a**). Values are mean ± SEM. n = 4–5 mice per group. c, Scoring of disease severity in chronic progressive MOG$_{35-55}$-induced EAE mice treated daily for ten days beginning at the peak of disease on day 15 (black arrow). n =12–16 mice per group. Graph depicts mean daily disease score ± SEM. **d**, Mean improvement of disease score (Δ) per animal (peak score minus ending score) of MOG$_{35-55}$ EAE cohort in (**c**). Also shown are external validation results in MOG$_{35-55}$ EAE from an independent contract laboratory. n = 12 mice per group. For all EAE experiments

drugs were dosed daily by intraperitoneal (i.p.) injection: clobetasol (2 mg/kg), miconazole (10 mg/kg), benztropine (10 mg/kg), or FTY720 (1 mg/kg). All EAE disease scoring was 0=no abnormality; 1=limp tail; 2=limp tail and hind limb weakness; 3=hind limb paralysis; 4=hind limb paralysis and forelimb weakness; and 5=moribund. Two-tailed t-test *p-value <0.05 and **p-value <0.01 for drug treated groups compared to their respective vehicle treated group. Source Data is provided for Figure 4a–d.